

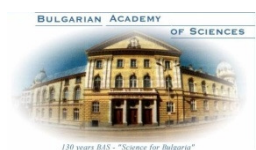
Ninth Workshop
Sunny Beach, Bulgaria, May 30 - June 3, 2017

N I N T H W O R K S H O P
**Solar Influences on the Magnetosphere,
Ionosphere and Atmosphere**

Sunny Beach, Bulgaria, May 30 - June 3, 2017



SPACE RESEARCH AND TECHNOLOGY INSTITUTE
BULGARIAN ACADEMY of SCIENCES



Scientific Organizing Committee

Katya Georgieva (Space Research and Technologies Institute, Sofia, Bulgaria) - Chair
Crisan Demetrescu (Institute of Geodynamics, Romanian Academy)
Ümit Deniz Göker (Bogazici University, Turkey)
Petra Koucka-Knizova (Institute of Atmospheric Physics, Czech Republic)
Vladimir Obridko (IZMIRAN, Moscow, Russian Federation)
Atila Özgüç (Kandilli Observatory, Turkey)
Jean-Pierre Rozelot (OCA-Lagrange, CNRS, Nice University, France)
Olga Malandraki (IAASARS, National Observatory of Athens, Greece)
Irina Mironova (Institute of Physics, St. Petersburg State University, St. Petersburg, Russia)

Topics:

Sun and Solar Activity
Solar Wind-Magnetosphere-Ionosphere Interactions
Solar Effects in the Ionosphere
Solar Influences on the Lower Atmosphere and Climate
Data Processing and Modelling
Instrumentation for Space Weather Monitoring

Local Organizing Committee:

(Space Research and Technologies Institute, Sofia, Bulgaria):

Boian Kirov - *Chair*;
Simeon Asenovski;
Dimitar Danov;
Rositsa Miteva



The workshop is partly supported by
the **National Bulgarian Science Fund**
N° ДПМНФ 01/16 (29 May 2017).

CONTENTS

Sun and Solar Activity

<i>Benghin V., Shurshakov V., Drobyshhev S., Semkova J., Mitrofanov I., Malahov A., Mokrousov M., Golovin D., Sanin A., and FRENDA team.</i> Comparison of Liulin-MO dosimeter radiation measurements during ExoMars 2016 TGO cruise to Mars and dose estimations based on galactic cosmic ray models	01
<i>Besliu-Ionescu D., Mierla M., Maris-Muntean G.</i> Study of CME-ICME properties during geomagnetic storms of SC 24	01
<i>Bojilova R., Mukhtarov P.</i> Influence of solar and geomagnetic activity on the ionosphere over Bulgaria	01
<i>Dechev M., Duchlev P., Koleva K.</i> Complex behavior of a solar prominence eruption	02
<i>Dineva E.I., Denker C., Strassmeier K.G., Ilyin I.</i> High-Resolution Sun-as-a-Star Spectroscopy with PEPSI/SDI	02
<i>Dorovskyy V., Melnik V., Konovalenko A., Brazhenko A., Rucker H.</i> Spatial properties of the complex decameter type II burst observed on 31 May 2013	03
<i>Georgieva K., Kilcik A., Nagovitsyn Yu., Kirov B.</i> On the ratio between the sunspot number and the sunspot group number	03
<i>Boychev B., Belyaev G., Kostin V., Ovcharenko O., Trushkina E.</i> Features of Upper Ionosphere Modification by Interactive Tropical Cyclons Based on Cosmos-1809 and Interkosmos Bulgaria-1300 Satellite Data.	04
<i>Ishkov V.N., Zabarinskaya L.P., Sergeeva N.A.</i> The collection and compile data on SPE for the period 19th -23rd cycles of solar activity	04
<i>Ishkov V.N.</i> From understanding principles to SPACE WEATHER forecast: experience of 3 solar cycles	05
<i>Dzhalilov N.S., Huseynov S.Sh.</i> MHD wave instability of anisotropic two-component solar wind plasma	05
<i>Kalinichenko N., Olyak M., Konovalenko A., Brazhenko A., Ivantishin O., Lytvynenko O., Bubnov I., Yerin S., Kuhai N., Romanchuk O.</i> A method for reconstructing the solar-wind stream structure beyond Earths orbit	05
<i>Kilcik A., Yurchyshyn V., Donmez B., Obridko V.N., Ozguc A., Rozelot J.P.</i> Temporal and Periodic Variations of Sunspot Counts in Flaring and Non-flaring Active Regions	06
<i>Kilcik A., Sahin S., Yurchyshyn V., Ozguc A.</i> Sunspot Group Variations after Flaring Activity	07
<i>Kirov B., Asenovski S., Georgieva K., Obridko V.N., .</i> On the Possibility to Predict the Future Sunspot Maximum	07
<i>Koleva K., Duchlev P., Dechev M.</i> Multi-wavelength Study of a Solar Two-ribbon Flare	07
<i>Koucka-Knizova P., Georgieva K., Mosna Z., Kozubek M., Kouba D., Kirov B., Potuznikova K., Boska J.</i> Solar periodicities detected within neutral atmospheric and ionospheric parameters	08
<i>Veselovsky I., Kaportseva K., Lukashenko A.</i> Eight types of the solar wind and their origins	08
<i>Maričić D., Roša Dr., Karlica M.</i> Heliospheric Observation of Earth-Directed Interplanetary Coronal Mass Ejection in 2008 - 2014	09

Ninth Workshop
Sunny Beach, Bulgaria, May 30 - June 3, 2017

<i>Melnik V., Brazhenko A., Dorovskyy V., Rucker H., Panchenko M., Frantsuzenko A., Shevchuk M. . Decameter type IV burst associated with behind-limb CME observed on November 7, 2013</i>	09
<i>Miteva R., Samwel S.W., Krupar V. . Solar radio burst emission from proton-producing flares and coronal mass ejections</i>	10
<i>Mosna, Z., Boska, J., Koucka Knizova, P., Chum J., Sindelarova, T., Kouba, D., Potuznikova, K.. Observation of the Solar Eclipse of 20 March 2015 at the Pruhonice station</i>	10
<i>Obridko V.N.. The solar dynamo and the relation of magnetic fields with different scale sizes.</i>	10
<i>Podgorny A.I., Podgorny I.M., Meshalkina N.S.. Magnetic Field Configuration in the Place of Solar Flare and Flare X-ray Sources</i>	11
<i>Podgorny I.M., Podgorny A.I.. Diagnostics of Solar Flares by Analyzing the Spectral Line Emission of Highly Ionized Iron</i>	11
<i>Mihajlović S, Cukavac M, Hasanagić E, Radovanović M, Milovanović B, Milenković M . Correlation between St. Patrick`s Day Geomagnetic Storm and Hurricane Nathan, 17 - 19 March 2015</i>	12
<i>Ryabov M.I., Sukharev A.L., Cycles and anti-cycles of solar activity and the basis for their prediction</i>	12
<i>Ryabov M.I., Volvach A.E., . Radio emission of activity complexes on the Sun in mm- and cm- waves.</i>	13
<i>Rozelot J.-P., Kosovichev A., Kilcik A. . How big is the Sun ? A critical assessment of the diameter data over the centuries.</i>	13
<i>Sahin S., Sarp V., Kilcik A.. Evolution and Life Time Variations of Flaring and Non-flaring Sunspot Groups</i>	14
<i>Semkova J., Krastev K., Dachev Ts., Koleva R., Malchev S., Tomov B., Matvichuk Y., Dimitrov P., Mitrofanov I., Malahov A., Golovin D., Bengehin V., and FRENDE team. Galactic cosmic rays radiation quantities onboard ExoMars Trace Gas Orbiter during the transit and in Mars orbit</i>	14
<i>Shepeliev V., Lytvynenko O.. Study of solar wind turbulence with interferometers URAN</i>	14
<i>Tashev V., Manev A.. Monitoring on the falling and accumulated solar energy on the Earth`s surface and forecasting for a period of one year with the help of automatic weather station.</i>	15
<i>Tsvetkov Ts.; Petrov N.. Kinematics of solar eruptive prominences according to space-based observations</i>	15
<i>Vernova E., Tyasto M., Baranov D.. Magnetic fields of the solar photosphere</i>	15
<i>Volvach Ya.S., Stanislavsky A.A., Konovalenko A.A., Koval A.A. . An upgrade of the UTR-2 radio telescope to a multifrequency radio heliograph</i>	16
<i>Werner R.. About the Causal Relationship between Global Temperature Anomalies and CO₂</i>	16
<i>Yankova Kr.. Unified model of the AGN</i>	16
<i>Zharkova V.V., Popova E., Shepherd S.J., Zharkov S.I.. Solar activity patterns derived from solar magnetic field with double dynamo model for dipole and quadruple sources</i>	17

Solar Wind-Magnetosphere Interactions

<i>Atici R., Sagir S.</i> , Comparison of Response to Severe Geomagnetic Storm of IRI and IONOLAB TEC Values	18
<i>Boska J., Kouba D., Koucka-Knizova P.</i> , Effects of geomagnetic activity observed in the ionospheric E and F region drifts measurements during the period 2005-2016 .	18
<i>Canyilmaz M., Yasar M., Güzel E.</i> , Noise Factor of the Different Modes of the Electromagnetic Waves Propagated in the Ionosphere	19
<i>Charkina O.V., Zalizovski A.V., Yampolski Yu.M.</i> , Diagnostics of Northern and Southern Auroral Ovals Using HF Signals on Superlong Radio Paths	19
<i>Demetrescu C., Dobrica V., Greculeasa, R.</i> , On the sources of the largest geomagnetic storms in solar cycles 23 and 24	19
<i>Despirak I.V., Lubchich A.A., Kleimenova N.G., Guineva V.</i> , Space weather conditions for the supersubstorm appearance	20
<i>Shagimuratov I., Chernouss S., Despirak I., Filatov M., Efshov I., Tepenitsyna N.</i> , Occurrence of TEC fluctuations and GPS positioning errors at different longitudes during auroral disturbance	20
<i>Dobrica V, Demetrescu C.</i> , Assessing the present trend in the heliosphere-magnetosphere-ionosphere system	21
<i>Gromova L.I., Gromov S.V., Kleimenova N.G., , Dremukhina L.A.</i> , Role of the IMF Bz / By in the Appearance of the Daytime High-Latitude Magnetic Bays	21
<i>Guineva V., Despirak I.V., Kozelov B., Werner R.</i> , Substorms over Apatity during the geomagnetic storm on 23 December 2014 –a case study	21
<i>Ishkova L., Ruzhin Yu., Bershadsкая I.</i> , The Large-Scale Ionosphere TEC Disturbances before Two Power Chilean Earthquakes.	22
<i>Manninen J., Turunen T., Kleimenova N., Rycroft M., Gromova L.</i> , Recently Revealed New Type of Daytime VLF Emissions Observed under Quiet Space Weather Conditions	22
<i>Lytvynenko O, Lytvynenko I.</i> , Comparison of Solar and Tropospheric Events Influence on Middle-Latitude Ionosphere Turbulence	23
<i>Ozcan O., Sağır S.</i> , The daily and seasonal variation of the ionospheric E-layer dynamo current	23
<i>Popova T.A., Yahnin A.G., Demekhov A.G.</i> , Comparison of EMIC Wave Observations in the Near-Equatorial Region of the Magnetosphere and Precipitation of Energetic Protons at Low Altitudes	24
<i>Sağır S., Atici R.</i> , Effect of CME and F10.7 solar flux on critical frequency value of Townsville F2 Region	24
<i>Sağır S., Ozcan O.</i> , Possible effect of stratospheric QBO on the ionospheric E-layer current	25
<i>Sarp V., Kilcik A.</i> , Solar Flare Effects on Geomagnetic Activity	25
<i>Semenova N.V., Yahnina T.A., Yahnin A.G., Demekhov A.G.</i> , The morphological characteristics of energetic proton precipitation equatorward of the isotropy boundary as measured by NOAA POES	25
<i>Sukharev A., Ryabov M., Orlyuk M., Romenets A.</i> , Dependence of global and regional geomagnetic disturbance on the state of solar activity in the 24th cycle.	26

Ninth Workshop
Sunny Beach, Bulgaria, May 30 - June 3, 2017

<i>Komendant V., Koshkin N., Ryabov M., Sukharev A.</i> Multiple correlation models of dependence of drag artificial satellites of the Earth on solar and geomagnetic activity in the 23 - 24th cycles.	26
<i>Vernova E., Tyasto M., Danilova O.</i> Planetary changes of cosmic ray cutoff rigidities in the maximum of the geomagnetic storm of November 2003	27
<i>Yaşar M., Canyilmaz M.</i> The Energy Barrier and Collision Number of O+ + H2(v=0, j=0) Reaction in the Earth Ionosphere	27
<i>Yesil A., Sağır S.</i> Calculation of Electric Field Strength (Ey) in the Ionospheric F-region	27
<i>Yesil A., Sağır S., Alisoy H.</i> Volume Polarization Tensor for Ionosphere E- Region in Northern Hemisphere	28
<i>Yesil A., Kurt K.</i> The integrated Coefficients of Diffusion Tensor for Ionosphere E-Region	28
<i>Yesil A., Sağır S.</i> Calculation of Electric Field Strength (Ey) in the Ionospheric F-region	28

Solar Influences on the Lower Atmosphere and Climate

<i>Erokhin N.S., Mikhailovskaya L.A., Zolnikova N.N., Artekha S.A., Shkevov R.</i> Dynamics analysis of the large-scale cyclogenesis for fast variations in background situation in cyclone region	29
<i>Kleimenova N., Michnowski S., Odzimek A., Kubicki M.</i> Space Weather Effects in Atmospheric Electric Field Variations	29
<i>Kozubek, M.</i> Long-term trends in the stratosphere	30
<i>Tashev V., Manev A.</i> Characteristic changes in the temperature of the atmosphere for different periods of time in the region of Stara Zagora	30
<i>Tonev P.</i> Transient variations in global electrical circuit caused by different factors and their relation to cloud formation	30
<i>Veretenenko S.</i> Comparative analysis of short-term effects of solar and galactic cosmic rays on the lower atmosphere circulation in the Northern hemisphere	31

Data Processing and Modelling

<i>Erokhin N.S., Shkevov R., Mikhailovskaya L.A., Zolnikova N.N., Artekha S.A.</i> Strong surfatron acceleration of helium nucleus by the electromagnetic wave in space plasmas	32
<i>Miteva R., Danov D.</i> On-line catalogues of solar energetic protons at SRTI-BAS	32
<i>Skokic I., Brajsa R., Sudar D., Kuhar M., Benz A.O.</i> Identification of features in solar ALMA images and comparison with solar atmospheric models	32
<i>Werner R., Petkov B., Valev D., Atanassov A., Guineva V., Kirillov A.</i> Determination of the total ozone column based on multi-dimensional lookup tables	33

Instrumentation for Space Weather Monitoring

<i>Semkova J., Koleva R. et.al.</i> Experiment Liulin-5: Review of the Measured Radiation Characteristics on Board the International Space Station	33
<i>Özgüc A., İsik S.</i> Temporal offsets between solar flare index and cosmic rays	34
<i>Barta M., Skala J., et.al.</i> Role of plasmoids in magnetic reconnection: Models and observations	34
<i>Barta M., Skokic I., Brajsa R. and the Czech ARC-node team</i> Solar research with ALMA: Czech node of European ARC as your user-support infrastructure.	34
<i>Klimov S., Grushin V. et.al.</i> The particularity of investigation of ELF-VLF electromagnetic radiation on sun-synchronous orbits. Project RELEC/Vernov.	35
<i>Kouba, D.</i> Comparison of Vertical Ionospheric Drifts Obtained by Different Techniques	35
<i>Obridko V.</i> Presentation of the book "Life and Universe"	35

Author's List	36
----------------------	----

Sun and Solar Activity

Comparison of Liulin-MO dosimeter radiation measurements during ExoMars 2016 TGO cruise to Mars and dose estimations based on galactic cosmic ray models

*Benghin V.¹, Shurshakov V.¹, Drobyshch S.¹, Semkova J.², Mitrofanov I.³, Malahov A.³,
Mokrousov M.³, Golovin D.³, Sanin A.³, and FRENDE team*

¹ State Scientific Center of Russian Federation, Institute of Biomedical Problems,
Russian Academy of Sciences, Moscow, Russia

² Space Research and Technology Institute, Bulgarian Academy of Sciences, Sofia, Bulgaria

³ Space Research Institute, Russian Academy of Sciences, Moscow, Russia

Flux and dose rate estimation on board ExoMars 2016 TGO have been made based on ISO/DIS 15390 galactic cosmic ray model and a new model developed recently in the Skobeltsyn Institute of Nuclear Physics of Moscow State University. The model of the Liulin-MO detectors shielding was created for calculations. The results have been compared with Liulin-MO dosimeter data. It is shown that tolerable agreement between experimental data and calculations is obtained if in the models is apply solar activity level (Wolf Number) smaller than observed.

Study of CME-ICME properties during geomagnetic storms of SC 24

Besliu-Ionescu D.¹, Mierla M.^{2, 1}, Maris-Muntean G.¹

¹ Institute of Geodynamics of the Romanian Academy

² Royal Observatory of Brussels

Most of geomagnetic storms (GS) are associated to solar activity. Their extensive investigation along with similar investigation of the correlated solar eruptive phenomena should lead to a better understanding of the causal chain

We will focus our study on moderate and intense geomagnetic storms ($Dst \leq -50$ nT) that were associated with interplanetary coronal mass ejections (ICME), which were clearly associated with their solar counterpart

We will present a detailed analysis of the coronal mass ejections (CME) properties and the interplanetary and geomagnetic conditions (B_z component of the interplanetary magnetic field and Dst) before and during geomagnetic storms for CME-ICME-GS associations from solar cycle 24

We will also present preliminary results of analysing Akasofu parameter temporal profiles in periods comprising the geomagnetic storms for the selected events

Influence of solar and geomagnetic activity on the ionosphere over Bulgaria

Bojilova R.¹, Mukhtarov P.¹

¹ National Institute of Geophysics, Geodesy and Geography-BAS

It was made an analysis of the seasonal dependence of the reaction of the maximum electron density of the ionosphere on the geomagnetic activity and the short-periodic variations of the ionizing solar radiation. The research was based on data from Ionospheric Station - Sofia from 1995 to 2014. Crosscorrelations and delay times between the relative values of the critical frequencies of the ionospheric F region with the planetary geomagnetic activity index K_p and the

Ninth Workshop

Sunny Beach, Bulgaria, May 30 - June 3, 2017

sun's radio emission wave with a wavelength of 10.7 cm for each calendar month of the year are investigated. The results can be used to create empirical models of ionospheric characteristics, depending of variations of solar and geomagnetic activity.

Complex behavior of a solar prominence eruption

Dechev M.¹, Duchlev P.¹, Koleva K.¹

¹ Institute of Astronomy & National Astronomical Observatory

We investigate the complex behavior of a prominence eruption on 2014 March 14. The eruptive event was observed by Solar Dynamic Observatory (SDO) at the eastern limb between 07:33 UT and 10:45 UT.

We used data from AIA/SDO and the two STEREO Observatories A and B.

The morphology and kinematics of the event was analysed on the base of 304 A and 195 A images.

The eruption shows a very complex evolution in which flux ropes interaction, magnetic reconnection, flare and prominence eruption were involved. The eruptive prominence eruption was observed in the LASCO C2 and C3 field-of-view as a bright core of partial halo CME and it can be traced up to 7.2 Rsun.

High-Resolution Sun-as-a-Star Spectroscopy with PEPSI/SDI

Dineva E.I.^{1 2}, Denker C.¹, Strassmeier K.G.¹, Ilyin I.¹

¹ Leibniz-Institute for Astrophysics Potsdam (AIP);

² University of Potsdam, Institute of Physics and Astronomy

The Potsdam Echelle Polarimetric and Spectroscopic Instrument (PEPSI) is a state-of-the-art, thermally stabilized, fiber-fed, high-resolution spectrograph for the 11.8 m Large Binocular Telescope (LBT) at Mt. Graham, Arizona. The Solar Disk-Integrated (SDI) is a small auxiliary telescope, which feeds sunlight to the spectrograph. Synoptic solar observations with PEPSI/SDI exploit the high photon flux of the Sun, producing daily spectra with high signal-to-noise ratio, providing access to unprecedented, quasi-continuous, long-term, disk-integrated solar spectra with high spectral and temporal resolution. These spectra contain a multitude of photospheric and chromospheric spectral lines in the wavelength range of 380 - 910 nm. We develop tools to monitor and study solar activity on different time-scales ranging from daily changes, over periods related to solar rotation, to annual and decadal trends. Strong chromospheric absorption lines, like the Ca II K & H lines, are powerful diagnostic tools for solar activity, since they trace the variations of the solar magnetic field. Currently, we are developing a data pipeline for extraction, calibration, and analysis of PEPSI/SDI data. We compare the SDI data with daily spectra from the Integrated Sunlight Spectrometer (ISS), which is part of the NSO Solar Long-Term Investigation of the Sun (SOLIS) facility. We present preliminary result for the Ca II K & H lines, including details of the wavelength and flux calibration, and discuss them in the context of synoptic full-disk images and magnetograms, linking spectral features to solar phenomena like sunspots, network fields, and filaments.

Spatial properties of the complex decameter type II burst observed on 31 May 2013

Dorovskyy V.¹, Melnik V.¹, Konovalenko A.¹, Brazhenko A.², Rucker H.³

¹ Institute of radio Astronomy, Kharkov, Ukraine

² Poltava Gravimetric observatory, Poltava, Ukraine

³ Space Research Institute, Graz, Austria

We present the results of observations of complex powerful type II burst associated with narrow Earth-directed CME, which was ejected at around 11 UT on 31 May 2013. The observations were performed by radio telescope UTR-2, which operated as local interferometer, providing the possibility of detection of the spatial parameters of the radio emission source. There are also polarization data from URAN-2 radio telescope.

The CME was detected by two space-born coronagraphs SOHO/LASCO/C2 and STEREO/COR1-BEHIND, and was absolutely invisible for STEREO-AHEAD spacecraft.

The associated type II burst consisted of two successive parts of quite different appearance on the dynamic spectrum. The first burst was narrow in frequency, had cloudy structure and was completely unpolarized while the second one represented rich herring-bone structure and exposed high degree of circular polarization. Both parts of the whole event reveal band splitting and well distinguished harmonic structure.

The sources of the type II bursts elements were found to be of about 15 arcmin in size in average, with the smallest ones reaching as low as 10 arcmin.

It was firstly found that sizes of the sources of herringbone sub-bursts rapidly increase with time. Such phenomenon was not observed for the cloudy part of the burst, what indicates that the accelerated electron beams may have different physical properties.

The work was partially performed under the support of the European FP-7 project SOLSPANET (F9P7-People-2010-IRSES-269299).

On the ratio between the sunspot number and the sunspot group number

Georgieva K.¹, Kilcik A.², Nagovitsyn Yu.³, Kirov B.¹

¹ SRTI-BAS, Sofia, Bulgaria

² Akdeniz University, Antalya, Turkey

³ Central Astronomical Observatory at Pulkovo, St. Petersburg, Russia

The sunspots are the most visible manifestation of solar activity, and with the longest data record. Two indices were until recently used to quantify the long-term evolution of solar activity: the International Sunspot Number R_z calculated from the number of sunspots and the number of sunspot groups, and the Group Sunspot Number R_g based on only the number of sunspot groups. The correlation between R_z and R_g is very high, but the ratio R_z/R_g is not constant leading to have differences between the two indices, mainly in their long-term trends. Since June 2015, the International Sunspot Number data series has been discontinued, and two new series were introduced for the sunspot number (S_n) and the sunspot group number (G_n) which now almost fully coincide and both has practically no long-term trends. Here we use data from three solar observatories (Learmonth, Holloman, and San Vito) to study the variations in the average number of sunspots per sunspot group. We find that the different types of sunspot groups and the number of sunspots in these groups have different solar cycle and cycle to cycle variations. Therefore, the varying ratio R_z/R_g is a real feature and not a result of changing observational instruments, observers experience, calculation schemes, etc. We show that these variations are a result of variations in the solar magnetic fields.

Features of Upper Ionosphere Modification by Interactive Tropical Cyclons Based on Cosmos-1809 and Interkosmos Bulgaria-1300 Satellite Data.

Boychev B.¹, Belyaev G.², Kostin V.², Ovcharenko O.², Trushkina E.²

¹ Institute of space research and technology of Bulgarian Academy of Sciences

² Institute of terrestrial magnetism, ionosphere and radio wave propagation RAS

The data analysis of the on-board instruments set of the Kosmos-1809 and IKB-1300 satellites is presented for the following events:

1. Sequences of 5 hurricanes in the Atlantic Ocean in September 1981.
2. Sequences of 3 super-typhoons in the Western Pacific in November 1990.
3. Continuous sequence of tropical cyclones (TC) after the Pinatubo and Hudson volcanoes eruption in 1991.

In July-December 1991, a continuous sequence of interacting typhoons was observed in the western part of the Pacific Ocean. Unique events developed on September 24, 1992, when eleven individual as well as interacting TC were registered on ten revolutions of the Cosmos-1809 satellite. It is shown that the effects of two interacting TCs impact on the ionosphere differ from those of single TCs. Self-organization of a single TC leads sequentially to the formation above it in the stratosphere of an anticyclone, and above - to a vertical flooded jet, which cause different effects in the ionosphere. If the developing of the first TC cause the second TC arise at a distance of ~ 20 degrees, the Ne structure and other plasma parameters of the upper ionosphere change. The strongest volcanic eruptions in the twentieth century (1991) threw a significant amount of aerosols into the stratosphere. Stratospheric changes for interacting TCs and perturbations after volcanic eruptions, apparently, cause a redistribution of infrasound along the TC track which can lead to the formation of a new TC.

The collection and compile data on SPE for the period 19th -23rd cycles of solar activity

Ishkov V.N.¹, Zabarinskaya L.P.², Sergeeva N.A.²

¹ IZMIRAN, Moscow, Troitsk, Russia

² GC RAN, Moscow, Russia

In the age of space exploration the promotion of scientific research on the solar active phenomena made it necessary to classify solar flare data, detect the sources and study the effects occurring in the Sun on the near-Earth space. The uniform representation for solar proton events (SPE) is particularly important. The sequence of catalogues provided 4 separate editions covers the period from 1970 to 2008 (20-23 solar cycles). The data on SPE with energy of $E > 10$ MeV exceeded $J_p \geq 1$ pfu are collected and systematized in these catalogues. In all publications of catalogues the same system for providing relevant information is accepted. In fact, this system is gradually increasing from publication to publication due to obtain complete and various information about solar flares, greater number of spacecrafts and improved research equipment. The last Catalogue in the 23rd SC (142 events) contains information on the particle sources, electromagnetic radiation, integral energy spectrum in the maximum of the proton flux for each SPE observed by several spacecraft. Each event is now illustrated by survey schedules of x-ray radiation, electron fluxes, speeds of solar wind, tension of interplanetary magnetic field and Dst-variations in near-Earth space in the time interval covering this event. A large volume of information in the Catalogues has demanded to implement improved and more modern methods of its presentation. For easy of reference the navigation tools were created in the catalogues allowing the user to move rapidly from the page `Contents` to the selected parts of the catalogue and back.

From understanding principles to SPACE WEATHER forecast: experience of 3 solar cycles

Ishkov V.N.
IZMIRAN, Troitsk, Moscow

Until 1989 an understanding was formed that practically all significant disturbance of Earth environment are caused exclusively by solar active phenomena: solar flare events and coronal holes. Became clear that flare processes arise as a result of the new emerging magnetic fluxes interaction with already existing magnetic fields. Observation of new magnetic fluxes emergence, estimation of their size and rate of emergence allows to predict the periods of significant solar flare events realization and to estimate degree their geoefficiency. The main agents, visualizing propagation of disturbance from solar flares and filament ejecta in a solar corona and in interplanetary space, are coronal mass ejections which parameters allow to estimate possible disturbances of the geomagnetic field, the growth of solar proton fluxes in near-earth space are. The forecast of recurrent geomagnetic disturbances and high fluxes of electrons ($E > 2$ MeV) in geostationary orbits is based on definition of the moment of an entrance of Earth to a solar wind high-speed stream from low latitude coronal. At present, it has been possible to understand that SA is divided into the epochs of `increased` and `lowered` SA that separated by transitional periods. Number of solar active phenomena and their manifestations in environment in all three classes of disturbances (R-S-G) for each epoch different, that one must take into account with the composition of forecasts. The current 24 cycle opened the second epoch `lowered` SA, which will be prolonged the following 4 SC and they will not be the cycles of high value.

MHD wave instability of anisotropic two-component solar wind plasma

Dzhalilov N.S.¹, Huseynov S.Sh.¹

¹ Shamakhy Astrophysical Observatory of ANAS, Azerbaijan

On the basis of 16-moment MHD transport equations we examined the propagation of linear waves in an anisotropic cosmic plasma. We obtained general dispersion equation taking into account two components of plasma (electrons and protons) and heat flux along magnetic field. Obtained dispersion equation is a generalization of earlier studied cases, when plasma is ionic. The case, when the effects related to heat flux are ignored was analyzed in detail. Within the limit of longitudinal propagation we gave a classification of wave modes which completely conforms to the known modes of kinetic physics of collisionless plasma. Fire-hose and mirror instabilities were analyzed. It is shown that the inclusion of electrons changes the instability criterion. The results are used to interpret the observed turbulence in the solar wind components.

A method for reconstructing the solar-wind stream structure beyond Earths orbit

*Kalinichenko N.¹, Olyak M.¹, Konovalenko A.¹, Brazhenko A.², Ivantishin O.³, Lytvynenko O.¹,
Bubnov I.¹, Yerin S.¹, Kuhai N.⁴, Romanchuk O.⁴*

¹ Institute of Radio astronomy of NAS of Ukraine, Kharkiv, Ukraine;

² Poltava Gravimetical Observatory, Poltava, Ukraine;

³ Karpenko Physico-Mechanical Institute of the NAS of Ukraine, Lviv, Ukraine;

⁴ Hlukhiv national pedagogical university, Hlukhiv, Ukraine

The interplanetary scintillation (IPS) observations at decameter wavelengths have a large potential. They allow the parameters and dynamic of the solar wind to be determined at different

Ninth Workshop

Sunny Beach, Bulgaria, May 30 - June 3, 2017

distances from the Sun (up to several a. u.). Since 80s such observations have been carried out with the URAN radio telescope system (including the largest in the world decameter radio telescope UTR-2, the frequency range 10 - 32 MHz), Ukraine. This report describes a new method for reconstructing the solar wind stream structure beyond Earth's orbit using two-station (UTR-2 and URAN-2 radio telescopes) interplanetary scintillation observations of compact radio sources at decameter wavelengths. The proposed method is based on Feynman path-integral technique for modeling theoretical IPS characteristics. The method has allowed the conclusion to be made that the solar wind beyond Earth's orbit is a collection of streams with different parameters (velocity, spectral index of the interplanetary turbulence spectrum, layer thickness). Analysis of experimental data showed the dynamic of such stream structure when the different solar wind flows replace each other on the line of sight to the radio source. The technique has the large potential for future investigations of the solar wind in whole Heliosphere. Our investigations, which throw light on the stream structure of the solar wind at the distances more than 1 a. u. (1 - 3 a.u.) from the Sun, are the first after the famous Ulysses mission.

Temporal and Periodic Variations of Sunspot Counts in Flaring and Non-flaring Active Regions

Kilcik A.¹, Yurchyshyn V.^{2,3}, Donmez B.¹, Obridko V.N.⁴, Ozguc A.⁵, Rozelot J.-P.⁶

¹ Akdeniz University Faculty of Science, Department of Space Science and Technologies, Antalya, Turkey

² Big Bear Solar Observatory, Big Bear City, CA 92314, USA

³ Korea Astronomy and Space Science Institute, Yuseong-gu, Daejeon, 305-348, South Korea

⁴ IZMIRAN, Troitsk, Moscow, Russia

⁵ Kandilli Observatory and Earthquake Research Institute, Bogazici University, Istanbul, Turkey

⁶ Université de la Côte d'Azur (OCA-CNRS) and 77, Ch. des basses Moulrières, Grasse (F)

We analyzed temporal and periodic behavior of sunspot counts (SSCs) in flaring (C, M, or X class flares), and non-flaring active regions (ARs) for the almost two solar cycles (1996 through 2016). Our main findings are as follows: i) The temporal variation of monthly means of daily total SSCs in flaring and non-flaring ARs are different and these differences are also varying from cycle to cycle; the second peak of flaring ARs are strongly dominant during current cycle 24, while this difference is not such a remarkable during cycle 23. The amplitudes of SSCs in the non-flaring ARs are comparable during the first and second peaks (maxima) of the current solar cycle, while the first peak is almost not existent in case of the flaring ARs. ii) Periodic variations observed in SSCs of flaring and non-flaring ARs are quite different in both MTM spectrum and wavelet scalograms and these variations are also different from one cycle to another; there are no meaningful periodicities in MTM spectrum of flaring ARs exceeding 45 days during solar cycle 24, while a 113 days periodicity detected from flaring ARs of solar cycle 23. For the non-flaring ARs the largest period is 72 days during solar cycle 24, while the largest period is 327 days during cycle 23.

Sunspot Group Variations after Flaring Activity

Kilcik A.¹, Sahin S.¹, Yurchyshyn V.^{2,3}, Ozguc A.⁴

¹ Akdeniz University Faculty of Science, Department of Space Science and Technologies,
Antalya, Turkey

² Big Bear Solar Observatory, Big Bear City, CA, USA

³ Korea Astronomy and Space Science Institute, Daejeon, South Korea

⁴ Kandilli Observatory and Earthquake Research Institute, Bogazici University, Turkey

The possible morphological variations observed on sunspot groups one day after the flaring activity were investigated for the time period of January 1996 through August 2016. Our main findings are as follows; 1) 75 % of all flaring sunspot groups are large and complex (D, E, F modified Zurich classes). 2) More than 50 % of A, B, and C groups changed morphologically, while the remaining groups (D, E, F, and H) did not change remarkably after the flare activity. 3) There is a significant increase in the sunspot group area of A, B, C, D, and H groups. Contrary, the sunspot group area of E and F groups show decrease after the flaring activity. 4) The sunspot counts of D, E, and F groups show decrease, while the A, B, C, and H groups show increase.

On the Possibility to Predict the Future Sunspot Maximum

Kirov B.¹, Asenovski S.¹, Georgieva K.¹, Obridko V.N.²,

¹ Space Research and Technologies Institute - BAS, Sofia, Bulgaria

² IZMIRAN Moskow, Russian

The influence of solar activity on the Earth's magnetic field has been studied for many years. It was found that there are two main factors causing geomagnetic storms: coronal mass ejections whose probability is proportional to the number of sunspots, and high speed solar wind streams. As the times of the sunspot maximum and the high speed solar wind streams maximum do not coincide, there are two geomagnetic activity maxima in each 11-year solar cycle.

In the present work we regard the Earth as a probe immersed in the solar wind, and based on the data for the time interval between the sunspot maximum and the geomagnetic activity maximum in the declining phase of the sunspot cycle n , and the value of the minimum geomagnetic activity in the beginning of sunspot cycle $n+1$, we forecast the maximum of cycle $n+1$.

Multi-wavelength Study of a Solar Two-ribbon Flare

Koleva K.¹, Duchlev P.¹, Dechev M.¹

¹ Institute of Astronomy and National Astronomical Observatory-BAS

A study of a two-ribbon flare preceded by a filament/prominence eruption is presented. The event was observed between 00:00 UT and 08:00 UT on 2014 february 18 in a quiet solar region.

The multi-wavelength analysis of the flare was made by data obtained from the Solar Dynamics Observatory (SDO). The kinematics and evolution of the ribbons were estimated using images in 131, 171, 195, 211 and 304 A EUV channels. The overlying magnetic fields evolution was examined by SDO/HMI data.

Solar periodicities detected within neutral atmospheric and ionospheric parameters

*Koucka-Knizova P.¹, Georgieva K.², Mosna Z.¹, Kozubek M.¹, Kouba D.¹, Kirov B.²,
Potuznikova K.¹, Boska J.¹*

¹ Institute of Atmospheric Physics, Czech Academy of Sciences, Prague, Czech Republic

² Space Research and Technology Institute, Bulgarian Academy of Sciences, Sofia, Bulgaria

We have analyzed time series of solar data together with the atmospheric and ionospheric measurements for solar cycles 19 till 23 according to particular data availability. For the analyses we have used long term data with 1-day sampling. By mean of Continuous Wavelet Transform (CWT) we have found common spectral domains within solar and atmospheric and ionospheric time series. Further we have identified terms when particular pairs of signals show high coherence applying Wavelet Transform Coherence (WTC). Despite wide oscillation ranges detected in particular time series CWT spectra we found only limited domains with high coherence by mean of WTC. Wavelet Transform Coherence reveals significant high power domains with stable phase difference for periods 1 month, 2 months, 6 months, 1 year, 2 years and 3 years between pairs of solar data and atmospheric and ionospheric data. The detected domains vary significantly during particular solar cycle (SC) and from cycle to the following one. It indicates the changing solar forcing and/or atmospheric sensitivity with time.

Eight types of the solar wind and their origins

Veselovsky I.^{1,2}, Kaportseva K.³, Lukashenko A.¹

¹ SINP MSU, Moscow, Russia

² IKI RAN, Moscow, Russia

³ Faculty of Physics, MSU, Moscow, Russia

In July 2016 high cadence data from the new DSCOVR satellite launched at the Lagrange point in February 2015 became available. On the basis of these data a binary (large-small) three-parameter classification of solar wind types according to the main hydrodynamic parameters (speed, density, temperature) is presented, and examples of the determination of different types of solar wind in real time are given. We get eight types of solar wind: hot-fast-dense, cold-fast-dense, hot-slow-dense, cold-slow-dense, hot-fast-rarefied, cold-fast-rarefied, hot-slow-rarefied, cold-slow-rarefied comparing to some average values for given time intervals. These types occur at different frequencies and are consequences of different solar activity sorts. The most interesting situations correspond to extreme values because of magnetospheric effects. This report considers possible solar `sources` of listed types depending from the averaging scale. `Sources` can be macroscopic or microscopic, dark or bright, dense or rarefied, etc. For their quantitative description the equations of MHD with dissipation or the plasma kinetics equations are used. In order to characterize and compare `sources` it is convenient to use dimensionless scaling analysis.

Heliospheric Observation of Earth-Directed Interplanetary Coronal Mass Ejection in 2008 - 2014

Maričić D.¹, Roša Dr.¹, Karlica M.²

¹ Astronomical Observatory Zagreb, Zagreb, Croatia.

² Sapienza University of Rome, Roma, Italia.

The relation between interplanetary coronal mass ejection (ICMEs) morphology and variety of phenomena occurring in the low corona, is still an open issue. Generally assumption is that all ICMEs have a flux rope structure, but some observational analyses shows that on average only one-third of detected ICMEs show clear magnetic cloud (MC) signature. Furthermore, existence of so-called stealth coronal mass ejection whose not exhibit any obvious low-corona signatures, clearly indicate necessity to upgrades of the theoretical ICME models. In this work we presented an online catalogue for general use of the Earth and near-Earth directed single ICMEs (ICMEs interaction are excluded) in the period from January 2008 to September 2014, with additional data of corresponding solar wind disturbance. ICMEs data are gathered from the Solar Terrestrial Relations Observatory (STEREO), Solar Dynamic Observatory (SDO) and Solar and Heliospheric Observatory (SOHO), although in situ data about solar wind are used from WIND satellite.

For all ICMEs we calculated kinematics parameters and for corresponding disturbances we made a detailed analysis of the in situ data. We separated the ICMEs in different types, regarding on their connections with low-corona signatures (especially: active region, prominence and flare). Our analysis shows that MC/flux rope structure is not recognised for ICMEs whose origin is not connected with obvious low-corona signatures.

Keywords. mass ejection, solar wind disturbance, prominence, flare

Decameter type IV burst associated with behind-limb CME observed on November 7, 2013

*Melnik V.¹, Brazhenko A.², Dorovskyy V.¹, Rucker H.³, Panchenko M.⁴,
Frantsuzenko A.², Shevchuk M.¹*

¹ Institute of Radio Astronomy, Kharkov, Ukraine

² Institute of Geophysics, Gravimetrical Observatory, Poltava, Ukraine

³ Commission for Astronomy, Graz, Austria

⁴ Space Research Institute, Graz, Austria

Results of observations of type IV burst (November 7, 2013) by the radio telescope URAN-2 (Poltava, Ukraine) in the frequency range 22-32 MHz, which accompanied by CME associated with a behind-limb active region with longitude -150 degree, are presented. This burst was registered also by STEREO A and B in the frequency range 8-14 MHz and by NDA (Nancy, France) in the frequency range 30-60 MHz. It was turned out to be a moving one with drift rate about 50 kHz/s in the band 22-32 MHz and apparently was generated by the accompanied CME. CMEs mass was $1.9 \cdot 10^{16}$ g that gave needed density for the generation of radio emission at frequencies 22-60 MHz with the help of plasma mechanism. The CMEs core was situated at distance about 2Rs at this time and it means that density in the core was significantly higher than the density of surrounded coronal plasma. Arguments in favor of the radiation at high frequency (60 MHz) escaped from the center of core and the radiation at low frequency (30 MHz) came out from circumferential regions are put forward. Type II burst and type III bursts, which were observed during type IV burst, and their connections with the CME are discussed also.

Solar radio burst emission from proton-producing flares and coronal mass ejections

Miteva R.¹, Samwel S.W.², Krupar V.^{3,4}

¹ Space Research and Technology Institute BAS, Bulgaria

² National Research Institute of Astronomy and Geophysics, Egypt

³ NASA/GSFC, USA

⁴ Institute of Atmospheric Physics CAS, Czech Republic

We present a statistical study on the radio emission signatures from flares and coronal mass ejections (CMEs) producing solar energetic proton (SEP) events. We utilize the Wind/EPACT proton event catalog over the period 1996-2016. Dynamic radio spectra from various ground based radio observatories and also from Wind/WAVES spacecraft have been analyzed. We identified the occurrence of radio burst types II, III, IV in several wavelength ranges and compared with observatory reports where available. Finally, we report on the solar cycle and longitude trends of the radio signatures associated with in situ proton events in view of the possibility to improve the existing SEP forecasting schemes.

Observation of the Solar Eclipse of 20 March 2015 at the Pruhonice station

*Mosna, Z., Boska, J., Koucka Knizova, P., Chum, J., Sindelarova, T.,
Kouba, D., Potuznikova, K.*

Institute of Atmospheric Physics, Czech Academy of Sciences

Response of the atmosphere to the Solar Eclipse on 20 March 2015 is described for mid-latitude region of Czech Republic. For the first time we show joint analysis using Digisonde vertical sounding, manually processed Digisonde drift measurement, and Continuous Doppler Sounding for the solar eclipse study. The critical frequencies foE, foF1 and foF2 show changes with different time offset connected to the solar eclipse. Digisonde drift measurement shows significant vertical plasma drifts in F2 region deviating from daily mean course with amplitudes reaching 15-20 m/s corresponding to the time of solar eclipse. Continuous Doppler Sounding shows propagation of waves in the NE direction with velocities between 70 and 100 m/s with a peak 30 minutes after first contact. We observed increased and persistent wave activity at heights between 150 and 250 km at time about 20 - 40 minutes after beginning of SE with central period 65 min.

The solar dynamo and the relation of magnetic fields with different scale sizes.

Obridko V.N.¹

¹ IZMIRAN, Moscow, Russia

Small-scale solar magnetic fields demonstrate features of fractal intermittent behavior, which requires quantification. For this purpose we investigate how the observational estimate of the solar magnetic flux density B depends on resolution D in order to obtain the scaling factor K in a reasonably wide range. The quantity K demonstrates cyclic variations typical of a solar activity cycle. In addition, k depends on the magnetic flux density. This scaling is typical of fractal structures. The obtained results trace small-scale action in the solar convective zone and its coexistence with the conventional large-scale solar dynamo based on differential rotation and mirror-asymmetric convection. Dynamo theory suggests that there are two types of solar dynamo, namely the conventional mean-field dynamo, which produces large- and small-scale magnetic fields involved in the activity cycle and also the small-scale dynamo which produces a

Ninth Workshop

Sunny Beach, Bulgaria, May 30 - June 3, 2017

cycle independent small-scale magnetic field. The relative contribution of the two mechanisms to solar magnetism remains a matter of scientific debate, which includes the opinion that the contribution of the small-scale dynamo is negligible. Here we consider several tracers of magnetic activity that separate cycle-dependent contributions to the background solar magnetic field from those that are independent of the cycle. Background fields are very poorly correlated with the sunspot numbers and vary little with the phase of the cycle. In contrast, the stronger magnetic fields demonstrate a pronounced cyclic behavior.

Magnetic Field Configuration in the Place of Solar Flare and Flare X-ray Sources

Podgorny A.I.¹, Podgorny I.M.², Meshalkina N.S.³

¹ Lebedev Physical Institute of the Russian Academy of Sciences

² Institute of Astronomy of the Russian Academy of Sciences

³ Institute for Solar-Terrestrial Physics SB of the Russian Academy of Sciences

X-ray and ultraviolet observations of solar flare and the absence of any significant changes of magnetic field on the photosphere during solar flare unequivocally show that flare energy release takes place in the solar corona. To define the solar flare mechanism which explain the fast energy release in the corona the MHD simulation in the corona above a real active region is performed. At setting conditions for MHD simulation no assumptions are done about the solar flare mechanism. All conditions are taken from observations. Magnetic field distribution observed on photosphere is used for setting boundary conditions. Results of MHD simulation above the active region AR 10365 show appearance of the current sheets in corona which positions coincide with positions of thermal soft X-ray sources of flares May 27, 2003 at 02:53 and May 29, 2003 at 00:51. Basing on MHD simulation results and observations the electrodynamic model of the flare is proposed. The flare energy is accumulated in the magnetic field of a current sheet in the corona. The magnetic field dissipation in the current sheet during instability causes plasma heating, and therefore the appearance of the thermal X-ray emission. The analyses of magnetic field configuration using specially developed graphical system show that the lines in the plane of the current sheet configuration, which are tangential to the projections of the magnetic field vectors on this plane, are very useful for presenting of the physical meaning of the processes of accumulation and rapid release of the flare energy.

Diagnostics of Solar Flares by Analyzing the Spectral Line Emission of Highly Ionized Iron

Podgorny I.M.¹, Podgorny A.I.²

¹ Institute of Astronomy RAS, Moscow, Russia

² Lebedev Physical Institute RAS, Moscow, Russia

The discovery of cosmic rays was the most revolutionary event in modern physics. The most popular cosmic ray acceleration mechanisms are shock waves. All these works are based on unproven assumptions. These assumptions are not confirmed by long-term observations. Information obtained from the world wide network of neutron monitors and measurements on GOES spacecraft demonstrates unambiguously that solar cosmic rays are accelerated in solar flares up to 20 GeV. Photos of the pre-flare state development and in the lines of highly ionized iron (SDO apparatus) indicate the accumulation of energy for a flare in the corona in a local (about 10^{10} cm) high temperature structure. The spectra of the accelerated proton observed with neutron monitors are formed during the decay of a current sheet. These phenomena are well described by the electrodynamic model of a solar flare, developed on the basis of observational data and numerical magnetohydrodynamical simulation using the initial and boundary

Ninth Workshop

Sunny Beach, Bulgaria, May 30 - June 3, 2017

conditions, taken from the active regions observation before the flare. A similar mechanism of proton acceleration has been observed in the laboratory studies of a powerful pulsed gas discharge (Artsimovich, 1958). Unfortunately, new observational data on solar flares are now absent due to the abnormally low activity of the Sun in the current solar cycle. The forecast of solar activity remains an unsolved problem. With the modern concept of cosmic rays, a fundamentally important question arises: can the mechanism of proton acceleration in solar flares explain the acceleration of particles of galactic cosmic rays.

Correlation between St. Patrick`s Day Geomagnetic Storm and Hurricane Nathan, 17 - 19 March 2015

*Mihajlović S¹, Cukavac M¹, Hasanagić E¹,
Radovanović M², Milovanović B², Milenković M²*

¹ Republic Geodetic Authority

² Geographical Institute `Jovan Cvijić` SASA

In the period from 17 to 19 March 2015, a solar storm was recorded in the solar activity, which was followed by development of the geomagnetic disturbance, that is, St. Patrick`s Day geomagnetic storm, which according to the characteristics of the variations of geomagnetic field belongs to a class of intense geomagnetic storms. Analyzing the relationship between indicators of the solar and geomagnetic activities and the wind speed in the hurricane Nathan (which appeared in this period), it has been found that there are statistically significant correlations. When viewing cross-correlations of mentioned parameters of the solar and geomagnetic activities on the one hand and the wind speeds in the hurricane Nathan on the other hand, the correlation increases, wherein the maximum correlation is achieved when the wind speeds are `shifted`, that is, when they lag 36 hours behind the indicators of the solar and geomagnetic activities.

Cycles and anti-cycles of solar activity and the basis for their prediction

Ryabov M.I.¹, Sukharev A.L.¹,

¹ Odessa observatory 'URAN-4' Institute of Radio Astronomy NASU

In previous works it was shown that the periodicity of the manifestation of solar activity in the northern and southern hemispheres of the Sun is essentially different and form the N and S cycles of activity. Among the detected differences of N and S cycles: the start and end time, the discreteness properties, the dynamics of the main periods, the time of the maxima, the periods of `faults` and `synchronization`. Further studies have shown that the time of absence of `spotless days` spots on daily data form the anti-cycles of activity of various dynamic manifestations in the northern and southern hemispheres. An obvious addition to the above cycles is the existence of coronal holes activity cycles. They are the main source of geomagnetic disturbances during the periods of minimum and phases of growth and decay of the solar cycle. The nature of the manifestation of the periodicity of N and S hemispheres from 12 to 24 cycles of activity is shown in the work. Each of the cycles contains different periods of variability and the forecasting of their activity should be carried out separately.

Radio emission of activity complexes on the Sun in mm- and cm- waves.

Ryabov M.I.¹, Volvach A.E.²,

¹ Odessa observatory 'URAN-4' Institute of Radio Astronomy NASU

² Crimean Astrophysical Observatory RAS

Activity complexes (CA) and complexes of active regions (CAR) on the Sun are among the largest scales in the manifestation of solar activity. Here are the most powerful manifestations of solar activity as a result of the interaction of various `cores` of activity inside the complex. Currently they are defined according to the data of cosmic orbiting solar observatories `SOHO` and `SDO` by UV and x-ray radiation in the corona. Radio maps of the Sun on millimeter and centimeter wavelengths allow the identification of CAO and CA and at lower levels in the chromosphere and the corona . This allows to connect a manifestation of activity from under photosphere levels convection zone to `magnetosphere` complexes in the solar chromosphere and Corona. In this paper, the technique of identifying complexes is presented and the dynamics of their activity in radio emission according to observation data of stations of the international Sun radio service `KRIM`: RT-22, RT-2, RT-3, PT-m (since 1957) in the Department of radio astronomy and Geodynamics of the Crimean Astrophysical Observatory, Metsahovi Radio Astronomy Observatory on RT-14 (37 Ghz), Radioheliographs Nobeyama(17 and 34 Ghz) and SSRT (Irkutsk, 5.1 Ghz). A feature of these data is that they allow to explore the dynamics of development of activity complexes from the 20th activity cycle when space observatories have not worked yet.

How big is the Sun ? A critical assessment of the diameter data over the centuries.

Rozelot J.-P.¹, Kosovichev A.², Kilcik A.³

¹ Nice-University, France

² New Jersey Institute of Technology, USA

³ Department of Space Science and Technologies, Akdeniz University, Antalya, Turkey,

The measurement of the solar diameter has a rich history extending well back into the past. Tackled by Greek astronomers from a geometric point of view, an estimate, although incorrect, has been first determined, not truly called into question for several centuries. A canonical value was adopted by Auwers in 1891. In spite of considerable efforts during the second half of the XXth century, involving dedicated space instruments, no consensus has been reached on this issue. However, a shrinking or an expanding shape is ultimately linked to solar activity, as gravitational or magnetic fields, which are existing mechanisms for storing energy during a solar cycle, lead to distinct perturbations in the equilibrium solar structure and changes in the diameter. We will here give a brief review of some of the most remarkable techniques used in the past, emphasizing the advent of high sensibility instruments on board satellites, such as SDO, which allows accurate determination of the shape of the Sun. Furthermore, notable features of the Near Sub-Surface Layer (NSSL), called the leptocline, can be established in relation to the solar limb variations, mainly through the shape asphericities coefficients. Recent studies encourage further in-depth investigations of the solar subsurface dynamics, observationally through SDO: we will show the latest results on such solar limb shape asphericities.

It turns out that such modern measurements are one of the ways we have now for peering into the solar interior, learning empirically about flows and motions there that would otherwise only be guessed from theoretical considerations.

Evolution and Life Time Variations of Flaring and Non-flaring Sunspot Groups

Sahin S.¹, Sarp V.¹, Kilcik A.¹

¹ Akdeniz University Faculty of Science, Antalya, Turkey

We investigated the observed morphological evolution and life time variations of sunspot groups (A, B, C, D, E, F, and H modified Zurich classes) separately for the flaring and non-flaring active regions for the time period of January 1996 through August 2016. Sunspot groups and Solar flare data used in this study are taken from National Oceanic and Atmospheric Administration (NOAA). In results of our analysis we found followings 1) In general, flaring sunspot groups have longer life time than the non-flaring ones. 2) Most of the flaring sunspot groups evolve to other classes, while the situation is opposite for the non-flaring ones during the observed period of time.

Galactic cosmic rays radiation quantities onboard ExoMars Trace Gas Orbiter

during the transit and in Mars orbit

*Semkova J.¹, Krastev K.¹, Dachev Ts.¹, Koleva R.¹, Malchev S.¹,
Tomov B.¹, Matvichuk Y.¹, Dimitrov P.¹, Mitrofanov I.², Malahov A.²,
Golovin D.², Begenhin V.³, and FRENDA team*

¹ Space Research and Technology Institute, BAS, Sofia, Bulgaria

² Space Research Institute, RAS, Moscow, Russia

³ State Scientific Center of Russian Federation, Institute of Biomedical Problems, RAS,
Moscow, Russia

Since April 2016 the dosimetric telescope Liulin-MO has been conducting radiation environment investigations aboard the Trace Gas Orbiter (TGO) of the joint ESA-Roscosmos mission ExoMars. Liulin-MO is a module of the Fine Resolution Epithermal Neutron Detector aboard TGO. Presented are data for the radiation dose rates, particle fluxes and dose equivalent rates of the galactic cosmic rays measured in the interplanetary space and in high elliptic Mars orbit in the phase of declining solar activity of 24-th solar cycle. Data obtained are compared to the data of other radiation measurements in the interplanetary space.

Study of solar wind turbulence with interferometers URAN

Shepeliev V.¹, Lytvynenko O.²

¹ IRA NASU, Kharkov, Ukraine

² IRA NASU, URAN-4, Odessa, Ukraine

The Ukrainian interferometer network URAN with baselines 42 to 960 kilometers was created to investigate the angular structure of space radio sources at decameter wavelengths. Inhomogeneities of electron density of the interplanetary plasma and Earth's ionosphere make a strong impact on accuracy of observations in this frequency range. At the same time a study of such influence provides important information on parameters of the scattering plasma on a propagation path of radio waves. To date, a large array of observational data have been collected during 23rd and 24th solar cycles with the URAN interferometers that can be used to probe the interplanetary plasma and the ionosphere. In this report we describe a method of analysis of the interferometer data and demonstrate its application for study of large-scale irregularities of the solar wind and search of footprints of influence of separate solar events on a turbulent condition of the solar wind.

Monitoring on the falling and accumulated solar energy on the Earth`s surface and forecasting for a period of one year with the help of automatic weather station.

Tashev V., Manev A.

Space Research and Technologies Institute - BAS

The amount of solar energy is measured in continuous mode every 15 seconds. For this purpose we use data obtained from sensors of solar radiation of meteorological station Vantage Pro 2 Plus. It is a semi-professional type, and one of its sensors is specifically designed for measuring solar radiation. The collected data from the sensor are integrated and recalculated in order to be obtained results for the solar energy that is absorbed for a certain period of time per unit Earth`s surface. The purpose of research is to trace how great is the repeatability during different periods. A high annual repetition provides a good opportunity to forecast energy yields in the coming years. The monitoring had been carried out for the region of Stara Zagora.

Kinematics of solar eruptive prominences according to space-based observations

Tsvetkov Ts.¹; Petrov N.¹

¹ Institute of Astronomy & National Astronomical Observatory-BAS

We tracked the behaviour of the prominence bodies during the eruptive process. Observations, obtained by two space-based instruments were used to study the plasma kinematics - Solar Dynamics Observatory/Atmospheric Imaging Assembly on heights up to 1.3 solar radii and Solar and Heliospheric Observatory/Large Angle and Spectrometric Coronagraph white-light coronagraph C2 on heights up to 6 solar radii. The presented height-time profiles of the eruptions show changes of the velocity of the prominence material.

Magnetic fields of the solar photosphere

Vernova E.¹, Tyasto M.¹, Baranov D.²

¹ IZMIRAN, SPb. Filial, St. Petersburg, Russian Federation;

² Ioffe Physical-Technical Institute, St. Petersburg, Russian Federation

Photospheric magnetic field distribution was studied using data of NSO Kitt Peak (1976 - 2003). Magnetic fields of different strengths (B) are concentrated in specific heliolatitude intervals. We distinguish four groups of magnetic fields of the strengths 0 - 5 G, 5 - 15 G, 15 - 50 G and B>50 G. These groups have drastically different latitudinal distributions and are connected with different solar activity manifestations. We find characteristic heliolatitudes (5 deg, 40 deg and 60 deg), which separate the localization regions for magnetic fields of various strengths. An essential feature of the photospheric magnetic field distribution is the imbalance between positive and negative magnetic fluxes. The sign of the imbalance of the magnetic flux in two polar regions (from 40 deg to the pole) coincides with the polar-field sign of the South hemisphere. The inverse picture can be seen for the sunspot zone: the sign of the imbalance of strong fields coincides with the polar-field sign of the North hemisphere. The imbalance between positive and negative fluxes of the sunspot zone correlates, on one hand, with the asymmetry of the magnetic field of the Sun-as-a-star and, on the other hand, with the sector structure of the interplanetary magnetic field.

An upgrade of the UTR-2 radio telescope to a multifrequency radio heliograph

Volvach Ya.S.¹, Stanislavsky A.A.¹, Konovalenko A.A.¹, Koval A.A.²

¹ Institute of Radio Astronomy, 4 Mystetstv St., Kharkiv, Ukraine

² Institute of Space Sci. and School of Space Sci. and Physics, Shandong Uni, Weihai, China

We present the broadband heliograph based on the UTR-2 radio telescope for obtaining the solar corona images in the frequency range 9-33 MHz with the frequency resolution 4 kHz, the time resolution up to 1 ms, and under the dynamic range about 90 dB. The instrument provides new possibilities to measure the non-thermal radiation in an unprecedented way for a better understanding of the radio emission processes in solar corona. We describe various aspects of the instrument including its antenna system, receiver front end, digital hardware and the data acquisition. This is the lowest-frequency heliograph operating in the world. It allows us to detect radio emission from solar radio sources in the upper solar corona near frequencies of ionosphere cut-off. The performance of the instrument is illustrated with source maps of solar radio bursts at low frequencies during the observational compaigns of 2013-2015.

About the Causal Relationship between Global Temperature Anomalies and CO₂

Werner R.

Space Research and Technology Institute, BAS, Stara Zagora, Bulgaria

The slowdown of the World economic development during the World War I, the Great Depression and the World War II lead to a deceleration of the CO₂ emissions. The adjusted global temperature determined by removal of temperature influences other than related to CO₂ follows close the CO₂ radiation term. The difference between the estimated adjusted temperature time evolution with and without the CO₂ slow down demonstrate very clear the close relation between the temperature change and the CO₂ radiative forcing. It is shown that the slowdown of the CO₂ emission in the period from 1939 up to 1950 and the related CO₂ concentration in the atmosphere, caused by human activities, generate a more slow increase of the temperature. Therefore CO₂ is the leading variable of the relationship between the global surface temperature and CO₂.

Unified model of the AGN

Yankova Kr.

Space Research and Technology Institute-BAS

In this paper will considering the an appropriate model for a unified description of active and sleeper cores and micro-quasars for completeness. To this aim will investigate the expansion of advective hypothesis in GR. Will analyze the behaviour on the emerging connections on the disk to the other components of quasars. We discuss development of the advective mechanism outside the disk.

Solar activity patterns derived from solar magnetic field with double dynamo model for dipole and quadruple sources

Zharkova V.V.¹, Popova E.², Shepherd S.J.³, Zharkov S.I.⁴

¹ Department of Mathematics, Physics and Electrical Engineering, Northumbria University, Newcastle upon Tyne, UK

² Nuclear Physics Institution, Moscow University, Moscow, Russia

³ School of Engineering, Bradford University, UK

⁴ Department of Physics and Mathematics, Hull University, Kingston upon Hull, UK

Applying Principal Components Analysis (PCA) to the full-disk synoptic maps of solar magnetic field variations in solar cycles 21-24 obtained by Wilcox Solar Observatory we derive a 4 pairs of eigen values and vectors (Zharkova et al, 2015) and the analytical expressions for the first pair (principal components) in two layers as the sums of periodic cosine functions. Extrapolation of the summary curve in the past 3000 years confirms the eight grand cycles of ~350-400-years superimposed on 22 year-cycles caused by beating effect of the two dynamo waves generated by dipole magnetic sources in the two (deep and shallow) layers of the solar interior. The summary curve has a remarkable resemblance to the sunspot and terrestrial activity reported in the past: the recent Maunder Minimum (1645-1715), Dalton minimum (1790-1815), Wolf minimum (1320), Homeric minimum (800-900 BC), the Medieval warmth period (900-1200), the Roman Warmth Period (400-10BC) and so on. Temporal variations of these dynamo waves are modelled with the two layer mean dynamo model with meridional circulation revealing a remarkable resemblance of the butterfly diagram to the one derived for the last grand minimum in 17 century, Maunder minimum, and predicting the one for the upcoming modern grand minimum in 2020-2055. Addition of the waves generated by quadruple magnetic sources in the inner layer allowed to recover Dalton minimum and the other minima of Glessberg's cycle.

Solar Wind-Magnetosphere Interactions

Comparison of Response to Severe Geomagnetic Storm of IRI and IONOLAB TEC Values

Atici R., Sagir S.,
Mus Alparslan University, Turkey

In this study, IRI (International Reference Ionosphere) and IONOLAB total electron content (TEC) values during severe geomagnetic storm on March 17, 2015 and June 22-23, 2015 are compared. The geomagnetic storm is determined by the solar (Bz, Vp and Np) and geomagnetic (Dst, Kp and Ap) indices. TEC values are obtained by IONOLAB model with GPS based and IRI-2012 model, which is an empirical model, in Ankara, Turkey. As a result of investigation, IRI-2012-TEC values (~ 38 TECu) are not change, while IONOLAB-TEC values increase significantly (~ 64 TECu) in the initial and main phase of the March 17, 2015 severe geomagnetic storm. In addition, maximum IONOLAB-TEC values decrease by 23 TECu during the return phase of the storm, but no change occur in IRI-2012 TEC values. During the severe geomagnetic storm on June 22-23, 2015, IONOLAB-TEC values in all phase of the storm show less change compared to the other storm. During both storms, it is seen that the IRI model predicts lower TEC values than the IONOLAB model before the storms, and generally higher predicts after the storm. Finally, it can be said that the IONOLAB model is more sensitive than the IRI-2012 model to the disturbances that occur at Ankara located in the middle latitude ionosphere during the severe geomagnetic storm.

Effects of geomagnetic activity observed in the ionospheric E and F region drifts measurements during the period 2005-2016 .

Boska J., Kouba D., Koucka-Knizova P.
Institute of Atmospheric Physics AS CR, Prague, Czech republic.

Modern HF digisonde DPS-4 D (Digisonde Portable Sounder), which is in operation at the Pruhonice observatory of the Institute of Atmospheric Physics, Prague (IAP) from 2004, enables us to carry out ionospheric drifts measurements. Using standard mode of automatic drift (autodrift mode) measurements the velocity of the F region drifts is usually determined in the vicinity of the peak of the electron density profile (N(h) profile). Since 2005 we are also measuring ionospheric drifts at the heights of the ionospheric E region (within the altitudinal interval of 95-145 km). Here we present the analysis of the plasma drifts of two different ionospheric regions observed under quiet time and under moderate-to-intense ionospheric storm conditions during the period 2005-2016. Storm effects on the electron density distribution are also presented.

Noise Factor of the Different Modes of the Electromagnetic Waves Propagated in the Ionosphere

Canyılmaz M., Yasar M., Güzel E.

Department of Physics, Firat University, 23169 Elazığ, Turkey

In this study, the noise factor of different modes of the electromagnetic wave travelling vertically in the ionosphere has been investigated. There is a slight decrease in the noise factor values near the 105 km and then a rise again for 4,5,6 MHz waves at all modes and equinox days. As the frequency of the wave increases, the noise factor values change periodically depending on the electron density.

Diagnostics of Northern and Southern Auroral Ovals Using HF Signals on Superlong Radio Paths

Charkina O.V.¹, Zalizovski A.V.¹, Yampolski Yu.M.¹

¹ IRA NASU

Auroral ovals represent areas in the high latitudes of the ionosphere in which a large number of protons, electrons and ions precipitate from the magnetosphere of the Earth. These particles have energies up to hundreds keV. The electric fields are intensive in the auroral zones, and field-aligned plasma irregularities are formed in these regions. The inhomogeneities are the cause of anisotropic aspect scattering of the HF radio emission.

In the Institute of Radio Astronomy of the National Academy of Sciences of Ukraine (IRA NASU) technique is developed for multiposition Doppler HF sounding of the ionosphere, in which HF broadcast stations and time signal radio stations are used as sources of a probe signal. IRA NASU Internet-controlled receiving points are situated in Arctic, Scandinavia, Europe, Africa and Antarctic.

The possibility of diagnostic of the auroral ovals using the superlong radio paths is demonstrated by data from Antarctic receiving position. The continuous registration of signals from station RWM of the Moscow Time and Frequency Service (55,75N, 38,2E) on Ukrainian Antarctic Station Akademik Vernadsky (UAS, 65,25S, 64,27W) is carried out from 2010. The recorded on UAS signals propagate along forward and backward radio paths as well as by scattering on the ionospheric irregularities of the auroral oval. Spectral and time selection of scattered mode allows to use this signal for determination of location of equatorial boundaries of the northern and the southern auroral ovals and for estimating the drift velocities of the ionospheric inhomogeneities in these regions.

On the sources of the largest geomagnetic storms in solar cycles 23 and 24

Demetrescu C., Dobrica V., Greculeasa, R.

Institute of Geodynamics, Romanian Academy

The largest geomagnetic storms in solar cycles 23 and 24, namely November 20, 2003, and March 17, 2015, respectively, are investigated from the perspective of their magnetospheric and ionospheric sources. The study is based on heliospheric magnetic field and solar wind data, on recorded one-minute geomagnetic data from the European geomagnetic observatories, and on appropriate geomagnetic indices. The contributions of the magnetospheric ring current and of auroral electrojets are quantitatively investigated to explain the observed geomagnetic field evolution at individual geomagnetic observatories.

Space Weather Conditions for the Supersubstorm Appearance

Despirak I.V.¹, Lubchich A.A.¹, Kleimenova N.G.², Guineva V.³

¹ Polar Geophysical Institute, Apatity, Russia

² Schmidt Institute of the Physics of the Earth RAS, Moscow, Russia

³ Space Research and Technology Institute, BAS, Stara Zagora, Bulgaria

Using the data of the SuperMAG global magnetometers network and data of the IMAGE magnetometers network we examine the particularly intense substorms (SML index < -2500 nT (it is similar to the AL index, but with greater longitudinal and latitudinal coverage) and AE index < -2500 nT), which could be called `supersubstorms` or SSS events. Solar wind and Interplanetary Magnetic Field (IMF) parameters have been taken from the OMNI database and catalog of the large-scale solar wind types (<ftp://ftp.iki.rssi.ru/omni/>). We conducted a comparative analysis of the space weather conditions of the appearance of 77 `supersubstorm` (SSS) events of which 72 were registered at SuperMAG network in 1998-2005 and 5 at IMAGE network in 2010-2016. It was found that the supersubstorms are mainly observed during the passage of magnetic clouds (MC, in 51.9%) and plasma compression regions before MC (so called SHEATH) - in 40.5%. The considered supersubstorms demonstrated the spatial-temporal dynamics similar to the `expanded` substorms, i.e. space-time propagation from the auroral geomagnetic latitudes.

Occurrence of TEC Fluctuations and GPS Positioning Errors at Different Longitudes During Auroral Disturbance

Shagimuratov I.¹, Chernouss S.², Despirak I.², Filatov M.², Efishov I.¹, Tepenitsyna N.¹

¹ West Department of IZMIRAN, Kaliningrad, Russia

² Polar Geophysical Institute, Apatity, Russia

We analyzed an occurrence of the GPS TEC fluctuations associated with auroral disturbances during January 7, 2015 storm and impact the disturbance on GPS precise positioning. We used auroral and subauroral GPS stations located at the European, American and Asian sectors. As measure of the TEC fluctuation activity was used the rate of TEC (ROT) and intensity fluctuations evaluated by index ROTI. We found a rather good consistency in the time evolution of substorms and intensity of the GPS fluctuations. The intensity of fluctuations was differed on longitude. It is associated with dependence TEC fluctuations occurrence on LT. The fluctuations are usually registered closely to the local midnight sector. During the storm maximal occurrence TEC fluctuations, we registered in all latitudinal sectors. Over Europe the auroral activity was occurred day time, so TEC fluctuations at this sector were weak than in American and Asian sectors. We have also analyzed an impact of the geomagnetic disturbances on the Precise Point Positioning errors. The positioning errors were determined using the GIPSY-OASIS software (APS-NASA). During the main phase of the storm we observed a significant increase of the positioning errors at auroral and subauroral GPS stations. The storm-time the 3D position error (P3D) reached the values more than 10 m, while during quiet time they did not exceed 10-20 cm. We found that the positioning errors to be correlated with the GPS ROTI intensity. We thank the Institutes who maintain the IMAGE Magnetometer Array, Grants of RFBR 16-05-01077, 17-45-510341, program № 7, PRAN.

Assessing the present trend in the heliosphere-magnetosphere-ionosphere system

Dobrica V, Demetrescu C
Institute of Geodynamics, Romanian Academy

The evolution of parameters describing the heliosphere-magnetosphere-ionosphere system is investigated from the view point of medium- and long-term variabilities. Based on certain measured data, as well as on some reconstructed parameters, we retrieve information for the last century (12 solar cycles #13-24). It seems that the evolution of the entire system, the present trend included, is a result of superposition of the two well known magnetic (Hale) and 80-90 year (Gleissberg) solar cycles.

Role of the IMF $|B_z|/|B_y|$ in the Appearance of the Daytime High-Latitude Magnetic Bays

Gromova L.I.¹, Gromov S.V.¹, Kleimenova N.G.^{2, 3}, Dremukhina L.A.¹

¹ IZMIRAN, Moscow, Troitsk, Russia

² IFZ RAS, Moscow, Russia

³ IKI RAS, Moscow, Russia

Solar wind-magnetosphere interaction manifests in different geomagnetic disturbances. We study several dayside magnetic bays observed at the IMAGE high-latitude stations in the post-noon sector under different IMF $|B_z|/|B_y|$ and IMF orientation. We found that when IMF $|B_z|/|B_y| < 1$, i.e. the IMF B_y magnitude dominated over the IMF B_z , the positive or negative magnetic bays appeared correspondingly to the IMF B_y sign both for northward and southward IMF B_z . Thus, the IMF B_y sign controlled the direction of the appropriate ionospheric current. We showed that under the positive IMF B_y the dawn convection vortex expanded to the afternoon sector, and the dusk convection vortex expanded to the pre-noon sector under the negative IMF B_y . The high-latitude field aligned currents (FACs) related to the ionospheric convection should increase in the near-noon sector that leads to an enhancement of the corresponding high-latitude ionospheric currents. Contrary to that, when the IMF B_z was more intensive than the IMF B_y , i.e. $|B_z|/|B_y| > 1$, the appearance of negative or positive dayside bays did not depend on the IMF B_y sign and more often controlled the IMF B_z sign. Such dayside bays could be mapped into the poleward expanding area of the ionospheric convection and upward FACs. We conclude that geomagnetic IMF effects in the dayside polar sector significantly depend on the IMF $|B_z|/|B_y|$ ratio.

Substorms over Apatity during the geomagnetic storm on 23 December 2014 –a case study

Guineva V.¹, Despirak I.V.², Kozelov B.², Werner R.¹

¹ Space Research and Technology Institute, Stara Zagora Department, Bulgaria

² Polar Geophysical Institute, Apatity, Russia

In this work we studied the substorms, observed over Apatity during the geomagnetic storm on 23 December 2014. This storm originated during complex interplanetary conditions and had a highly structured recovery phase. Measurements from the Multiscale Aurora Imaging Network (MAIN) in Apatity have been used. Solar wind and interplanetary magnetic field parameters were taken from the OMNI data base. Substorm onset and further development were verified by the IMAGE magnetometers latitudinal chain and by data of the all-sky camera at Apatity.

Ninth Workshop

Sunny Beach, Bulgaria, May 30 - June 3, 2017

9 substorms were identified from 24 to 27 December 2014: 2 substorms in the main storm phase and 7 - during the structured recovery phase.

An attempt is made to connect these events to the magnetospheric phenomena based on satellite data. Themis measurements were used to verify the magnetic reconnection and the particles energy fluxes at the storm time. The orbits of Themis D and Themis E, located in the near Earth plasma sheet, were mapped from the magnetosphere to the ionosphere along the magnetic field lines and it was found that they crossed Cola peninsula during the time interval 24-27 December 2014 from about 18:30 to 19:30 UT. Some substorms on 24, 25 and 26 December 2014 were registered in this time interval or close after it. The energy fluxes, electric and magnetic field data were examined..

The Large-Scale Ionosphere TEC Disturbances before Two Power Chilean Earthquakes.

Ishkova L., Ruzhin Yu., Bershadskaya I.

Pushkov Institute of Terrestrial Magnetism, Ionosphere and Radio Wave Propagation of Russian Academy of Sciences, IZMIRAN

The analysis results of the large-scale space-time variations of the total electron content (TEC) of the South American ionosphere before the powerful Chilean earthquakes in February 27, 2010 (M=8.8) and in April 1, 2014 (M=8.2) are presented.

The daily TEC variations was analyzed in the periods 17–27.02.2010 and 25.03–03.04.2014 in comparison with the ten-day medians ($\delta\text{TEC},\%$, local time interval is 2 hours) in the longitudes $30^\circ\text{--}105^\circ\text{W}$ ($\Delta\lambda=15^\circ$) and in the latitudes $20^\circ\text{N--}60^\circ\text{S}$ ($\Delta\phi=5^\circ$). It was studied the development in the quiet geomagnetic conditions of the anomalous disturbances in the daily TEC in the extended ionosphere regions over the Andean seismic zone.

It was noted the development of the strong positive TEC disturbances (from 30 to 50÷60 % and higher) at the distances of up to several thousand kilometers (comparable to Dobrovolsky radius) for a few days before these earthquake main shocks. Near 3-4 days before the main shocks the passage from the positive TEC disturbances to the negative disturbances was occurred.

The maximum characteristics of the positive disturbances (values $\delta\text{TEC}, \%$ and their durations and direction distances) are higher than the same negative characteristics. The maximum durations of the positive disturbances (to 5–7 hours at night and morning) was noted in the latitudes $\sim 20\text{--}40^\circ\text{S}$. The durations of the negative TEC disturbances were 1-3 hours.

The correspondence of δTEC variation character to the space-time pattern of the seismic activity in the Andean seismic zone was noted.

Recently Revealed New Type of Daytime VLF Emissions Observed under Quiet Space Weather Conditions

Manninen J.¹, Turunen T.¹, Kleimenova N.², Rycroft M.³, Gromova L.⁴

¹ Sodankylä Geophysical Observatory, Sodankylä, Finland

² Institute of the Physics of the Earth, Moscow, Russia

³ CAESAR Consultancy, Cambridge, UK

⁴ IZMIRAN, Moscow, Troitsk, Russia

The natural electromagnetic waves at audio frequencies termed Very Low Frequency (VLF) emissions are typically generated in the magnetosphere via the electron-cyclotron resonance mechanism. These whistler-mode waves are guided to the ionosphere by the geomagnetic field with the upper cut-off frequency at half of the equatorial electron gyrofrequency ($f_{ce}/2$) at a given L-shell. Based on the VLF signals observed in Northern Finland at Kannuslehto (KAN, L~

Ninth Workshop

Sunny Beach, Bulgaria, May 30 - June 3, 2017

5.5, $f_{ce}/2 \sim 2.5$ kHz), recently we revealed a new and previously unknown daytime type of VLF-emissions at frequencies well above 4-5 kHz. These emissions have never been seen before because they were hidden by strong impulsive sferics originating in lightning. The peculiar VLF signals, discovered after filtering out the sferics, were studied. It is shown here that these emissions, which have a complicated spectral structure, occur during the winter around local noon under quiet solar and geomagnetic conditions ($V_{SW} < 400-500$ km/s, $B_{IMF} < 5-7$ nT, $N_p < 5-8$ cm⁻³, $AE < 150-200$ nT). We suppose that these waves are generated deep into the magnetosphere at much lower L-values than KAN. However, the details of the generation and propagation mechanisms of these newly discovered VLF emissions remain unclear.

Comparison of Solar and Tropospheric Events Influence on Middle-Latitude Ionosphere Turbulence

Lytvynenko O., Lytvynenko I.

Institute of Radio Astronomy of NASU

As is known, both space weather and subjacent atmosphere have influence on a ionosphere condition. In particular it concerns to ionosphere turbulence. As a rule, the authors consider separately solar and atmospheric effects on ionosphere. Ours comparative analysis of ISME and tropospheric fronts influences on ionosphere turbulence was carried out on the base of observation data obtained on radio telescope URAN-4 (Odessa, Ukraine) during 1998-2001 years at frequencies of 20 and 25 MHz. The extent of turbulence can be characterized by the intensity of the ionosphere scintillation of compact cosmic radio sources. After preliminary processing we had statistical sample in volume out 540 of daily average scintillation indices. It is reasonable value for such task.

The Daily and Seasonal Variation of the Ionospheric E-layer Dynamo Current

Ozcan O., Sagir S.

Firat University, Department of Physics

In the ionospheric E-layer, thermospheric winds and electric field cause the ions and electrons to drift in different directions. These drifts set up a current which produces ground-level geomagnetic field variations. The quite daily geomagnetic field variations are primarily due to the dynamo currents flowing in the ionospheric E-layer. For this reason, it is important to know the daily and seasonally variations of the ionospheric E-layer dynamo current. We have obtained the general expression of height-integrated conductivity and the current density for the ionospheric plasma; by solving the equation

for charged particles. The numerical values of these parameters have been calculated by using the ionospheric parameters which were obtained by the International Reference Ionosphere (IRI) model. The current densities calculated at different geographical latitudes have been examined daily and seasonally. The current density was examined separately for the days when the sun spot was maximum and minimum. Daily and seasonal variations of current density have been examined separately for maximum and minimum sunspot number.

Comparison of EMIC Wave Observations in the Near-Equatorial Region of the Magnetosphere and Precipitation of Energetic Protons at Low Altitudes

Popova T.A.¹, Yahnin A.G.², Demekhov A.G.³

¹ Polar Geophysical Institute, Apatity, Russia

² Polar Geophysical Institute, Apatity, Russia

³ Institute of Applied Physics RAS, Nizhny Novgorod, Russia

We study conjugacy of the generation region of EMIC waves with energetic proton precipitation by using wave data from THEMIS spacecraft and energetic proton data from low-orbiting NOAA POES and MetOp satellites. For this study we developed a plug-in for SPEDAS software ensuring proper comparison of the observations onboard magnetospheric and low-altitude spacecraft. The plug-in calculates the projections of spacecraft orbits on the ionospheric altitude (100 km) in the SM coordinate system (by using the IGRF model for low-altitude spacecraft and different versions of the Tsyganenko models for magnetospheric spacecraft). For close projections the latitudinal distributions of the compared parameters from different spacecraft are built. In our case, these parameters are the precipitated energetic proton fluxes measured by the NOAA POES and MetOp, and EMIC wave intensity from THEMIS. The wave intensity is calculated separately for H⁺ and He⁺ bands. The frequencies corresponding to the maximum spectral amplitudes of the waves are determined in each band. The latitudinal distribution of the density of the cold plasma in the magnetosphere is built where possible. The conjugacy of the regions of EMIC wave generation and energetic proton precipitation is most clearly seen for the events related to quasi-monochromatic Pc1 emissions whose source does not change its latitudinal position for sufficiently long time. We show that the proton precipitation accompanies the EMIC wave generation in both He⁺ and H⁺ bands. In this case, the EMIC waves below/above the He⁺ gyrofrequency usually occurs in the plasmasphere/outside the plasmapause.

Effect of CME and F10.7 solar flux on critical frequency value of Townsville F2 Region

Sağır S.¹, Atıcı R.²

¹ Department of Electronics and Automation, Vocational School, Mus Alparslan University, Mus, Turkey

² Faculty of Education, Mus Alparslan University, Mus, Turkey

In this study, the effect of Coronal Mass Injection (CME) and F10.7 solar flux on the foF2 values obtained from SPIDR during period 01.01.1986-31.12.2008 at Townsville station (19.7 S, 146.9 E) has been investigated. The statistical multiple regression model has used for the analysis. It has observed that about 78% of the changes occurring in foF2 at the end of the investigation can be explained by the solar CME and F10.7 solar flux indices. An increase 1W/sr in the CME causes an increase 0.21 MHz in the foF2 critical frequency value. Also, an increase of 1 s.f.u. in the F10.7 solar flux appears to cause an increase of 0.0021 MHz in the foF2 critical frequency value. Based on these results, it can be said that both CME and F10.7 solar flux have a positive effect on in foF2 and that the effect of CME on foF2 is 100 times more than the effect of F10.7 solar flux.

Possible effect of stratospheric QBO on the ionospheric E-layer current

Sağır S.¹, Özcan O.²

¹ Mus Alparslan University

² Fırat University

It is known that ionospheric winds cause the ions to drift in the geomagnetic field. This drift set up a current which produces ground-level geomagnetic field variations. In this study, the relationship between stratospheric QBO and the ionospheric E- region current densities (J_x and J_y) for low latitudes (01.22 N, 103.55 E) have been statistically investigated. Also the effect of F10.7 solar flux index was included in the investigation. As a result of the investigation using the multiple regression model, it was determined that an increase of 1 s.f.u in the F10.7 solar flux caused an increase of 2.5×10^{-2} A / km on both J_x and J_y current density, while an increase of 1 m / s in the QBO caused a decrease of 2.1×10^{-3} A / km and 4.6×10^{-3} A / km on J_x and J_y current densities, respectively.

Solar Flare Effects on Geomagnetic Activity

Sarp V.¹, Kilcik A.¹

¹ Akdeniz University Faculty of Science, Department of Space Science and Technologies,
Turkey

We have analyzed the relationship between Solar Flare activity and geomagnetic indices such as AE index, aa index, CME speed index. As a flare activity data we used two time series, which are monthly flare energy and monthly flare number. Temporal variations and correlations between solar and geomagnetic activity indices were studied. To remove short term fluctuations and reveal the long term trends all monthly data sets were smoothed by 12 step running average for the temporal variation. We have found following results; 1) Flare number data are exactly following solar activity, while flare energy shows serious deviations especially of solar cycle 23. Contrary, both data are following each other quite well during solar cycle 24. 2) All geomagnetic activity indices access to their maxima in the middle of 2003 during solar cycle 23, while solar indices access to their maxima in the middle of 2001. Similarly, geomagnetic indices access to their maxima later than the solar indices except maximum CME speed index. 3) Solar flares and geomagnetic activity indices are highly correlated but a time delay is present at some geomagnetic indices.

The morphological characteristics of energetic proton precipitation equatorward of the isotropy boundary as measured by NOAA POES

Semenova N.V.¹, Yahnina T.A.¹, Yahnin A.G.¹, Demekhov A.G.^{1 2}

¹ PGI, Apatity, Russia; ² IAP RAS, Nizhny Novgorod, Russia

On the basis of NOAA POES observations we constructed a map of the global occurrence rate of energetic proton precipitation (EPP) equatorward from the isotropy boundary. It is shown that the occurrence rate of EPP within anisotropy zone is maximal in the afternoon sector at $L=6-9$ and decreases to dawn and dusk. There is a tendency to growth of the occurrence rate with the increase of solar wind dynamic pressure and geomagnetic activity. We compared the global distribution of EPP with observational statistics of EMIC waves revealed from magnetospheric spacecraft data, and found the remarkable similarity. This confirms that EPP events are the result of the ion-cyclotron instability in the equatorial magnetosphere.

Dependence of global and regional geomagnetic disturbance on the state of solar activity in the 24th cycle.

Sukharev A.¹, Ryabov M.¹, Orlyuk M.², Romanets A.²

¹ Radio Astronomy Institute NAS of Ukraine

² Geophysics Institute NAS of Ukraine

Examined relationship in manifestations of geomagnetic disturbance according digital measurements data from magnetic observatories in Kiev and Odessa cities, with global processes determined by the manifestations of solar activity in the 24th cycle. Measurement conditions at Odessa magnetic observatory differ from the measurements in Kiev, by presence of magnetic anomaly in this region, which may have a special response to solar activity. In the early works, on basis of continuous wavelet analysis, main short-period components of the magnetic field perturbation (2008 - 2015 years) characteristic for two stations (24, 12, 8, 6 hours) were presented. In the Odessa data, periods of 4 and 5 hours are additionally noted. For the short-period component in different seasons of the year, there are changes in periods. The identification of long-term variability by Fourier filtering and reconstructions shows existence for Odessa, periods of 84, 37, 17, 10 days. For Kiev, the periods of 87 and 50 days are more characteristic. The periods, indicated above, observed on background of planetary geomagnetic disturbances, dynamics of which were determined on basis of wavelet analysis according to daily Ap indices for medium latitudes. Also reported about planned program for monitoring state of magnetic field in region of magnetic anomaly at location of radio telescope URAN-4, for comparison with data of Odessa magnetic station located outside this zone.

Multiple correlation models of dependence of drag artificial satellites of the Earth on solar and geomagnetic activity in the 23 - 24th cycles.

Komendant V.¹, Koshkin N.¹, Ryabov M.², Sukharev A.²

¹ Odessa I.I. Mechnikov National University

² Radio Astronomy Institute NAS of Ukraine

The calculation of multiple correlation models determining the dependence of drag dynamics of 15 satellites on circular and elliptical orbits on the parameters of solar and geomagnetic activity is made. The processed information includes: declining and minimum phases of 23-rd (2005÷2008) solar cycle; phases of rise and maximum of 24-th (2009÷2014) solar cycle. For the analysis the following indexes were taken: W –Wolf numbers; Sp –the total area of sunspot groups of the northern and southern hemispheres of the Sun, F10.7 –the solar radio flux at 10,7 cm; E –electron flux with energies more than 0,6 MeV÷2 MeV; planetary, high latitude and middle latitude geomagnetic index Ap. For satellites in circular orbits, the values of the multiple correlation coefficient varied within 0.75-0.87. For satellites in elliptical orbits, the coefficient of multiple correlation varied from 0.15 to 0.65. The greatest contribution to the dynamics of deceleration was made by changes in the flux of radio emission at a wavelength of 10.7 cm, changes in Wolf numbers and total areas of groups of spots.

Planetary changes of cosmic ray cutoff rigidities in the maximum of the geomagnetic storm of November 2003

Vernova E., Tyasto M., Danilova O.
IZMIRAN, SPb. Filial, St. Petersburg, Russian Federation

Changes in the magnetic field of the magnetosphere under the action of solar wind lead to a redistribution of fluxes of charged particles of cosmic rays (CR), including the fluxes reaching the atmosphere boundary and surface of the Earth. Vertical cosmic ray cutoff rigidities were calculated for the minimum of the Dst-variation on November 24, 2003 for world grid 5x15 deg. For these purposes the CR particle trajectory tracing method in the magnetic field of the Tsyganenko disturbed magnetosphere model Ts01 was used. The results were compared with cutoff rigidities of Shea and Smart for IGRF2000. The areas of the large differences between them are revealed.

The Energy Barrier and Collision Number of O⁺ + H₂ (v=0, j=0) Reaction in the Earth Ionosphere

Yaşar M., Canyılmaz M.
Department of Physics, Firat University, 23169 Elazığ, Turkey

In this work, we discussed the effect of collisions of O⁺+H₂→OH⁺+H reactive reaction on the Earth ionosphere. The reaction rate constant and total cross sections which are calculated as a function of altitude have been used. Also all the parameters related with the ionosphere are calculated for the 38.40 N, 39.12 E coordinates and year, day and time are taken as 2009, equinox, local time (12:00) respectively. It was shown that the reaction rate constant and cross section values are decreasing with ionospheric height. The total collision number between O⁺ and H₂ takes the maximum values at the lower ionosphere and decreases with increasing height in upper ionosphere. The energy barrier is much closed to each other for all months and increased with the altitude.

Calculation of Electric Field Strength (E_y) in the Ionospheric F-region

Yesil A.¹, Sağır S.²

¹ Department of Physics, Faculty of Sciences, Firat University, 23119 Elazığ, Turkey

² Department of Electronics and Automation, Mus Alparslan University, Mus, Turkey

In this study, we have calculated the electric field strength (E_y) becoming a plane electromagnetic wave with frequency f , propagation along z-axis and the polarized along y-axis in one dimension by using WKB (Wentzel, Kramers and Brillouin) method and has considered for both collisional and without collision conditions in ionospheric F-region with regard to seasonal and local time. Also the refractive index of ordinary wave and attenuation factor have computed not only collisional but also collisionless case for the considered conditions. It is possible that when the collisions have calculated in F region of ionosphere, the electric field strength decrease for all season and E_y increases between 275-400 km altitudes encountering approximately hmF₂ "the peak of F₂" for the accepted conditions.

Volume Polarization Tensor for Ionosphere E- Region in Northern Hemisphere

Yesil A. ¹, Sagir S. ², Alisoy H. ³

¹ Department of Physics, Faculty of Sciences, Firat University, Elazig, Turkey

² Department of Electronics and Automation, Vocational School, Mus Alparslan University, Mus, Turkey

³ Electrical engineering, Engineering Faculty, Namik Kemal University, Tekirdağ, Turkey

We have calculated volume polarization (VP) tensor for ionosphere E- region by using the real geometry of Earth's magnetic field for in northern hemisphere at equinox days for both geographic latitude and local time. It could considerably say from results of findings that the diagonal elements of VP are same phase externally applied electric field and other elements in opposite phase vibrate for the accepted conditions. The whole elements of VP are approximately maximum around equator and at 12.00 LT. We can say that the diagonal elements of tensor are to show a capacitive behavior at equator

The integrated Coefficients of Diffusion Tensor for Ionosphere E-Region

Yesil A. ¹, Kurt K. ²

¹ Department of Physics, Faculty of Sciences, Firat University, Turkey

² MEB, Competition Authority Anatolian High School, Physics Teacher, Diyarbakir, Turkey

In this context, we investigated the integrated of diffusion tensor with geographic latitudes for equinox days (March 21 and September 23) at ionospheric E-region (110 km). The integrated diffusion values don't change both March 21 and September 23, 12:00÷24:00 LT for 1990 year. It is possible say that the geographic latitude becoming sharply decrease and increase "abnormal case" is equatorial anomaly region. For this reason, we think that this abnormal case could result from the equatorial anomaly in ionospheric E-region.

Calculation of Electric Field Strength (Ey) in the Ionospheric F-region

Yesil A. ¹, Sağır S. ²

¹ Firat unv. Department of Physics.,

² Mus Alparslan univ. Mus, Turkey

In this study, we have calculated the electric field strength (Ey) becoming a plane electromagnetic wave with frequency, propagation along z-axis and the polarized along y-axis in one dimension by using WKB (Wentzel, Kramers and Brillouin) method and has considered for both collisional and without collision conditions in ionospheric F-region with regard to seasonal and local time. Also the refractive index of ordinary wave and attenuation factor have computed not only collisional but also collisionless case for the considered conditions. It is possible that when the collisions have calculated in F region of ionosphere, the electric field strength decrease for all season and Ey increases between 275-400 kilometers altitudes encountering approximately hmF₂, the peak of F₂, for the accepted conditions.

Solar Influences on the Lower Atmosphere and Climate

Dynamics analysis of the large-scale cyclogenesis for fast variations in background situation in cyclone region

Erokhin N.S.^{1, 2}, Mikhailovskaya L.A.¹, Zolnikova N.N.¹, Artekha S.A.¹, Shkevov R.³

¹ Space Research Institute Russian Academy of Scienc

² Peoples Friendship University of Russia

³ Space Research and Technology Institute - Bulgarian Academy of Sciences

Small parametric model (SPM) based on a system of nonlinear differential equations for the maximum wind speed and ocean surface temperature in the typhoon zone presented. An analysis of large-scale processes dynamics in an atmosphere such as tropical cyclones (TC) was done. The generalized nonlinear model containing time depending free parameters. By variations in their choice can be controlled temporal dynamics simulations of regional cyclogenesis, in particular, changing the number of typhoons formed in a given region during the active season and their characteristics. Process of the large-scale TC dynamics resulting to the formation of three typhoons with different lifetime was considered. The calculations has shown that short-life TCs are less sensitive to small changes in background conditions than long-life ones, compared to the period of variations in the background situation. Various external factors necessary to take into account, for example, the influence of solar radiation, the role of solar-terrestrial connections and the effect of atmosphere ionization by cosmic rays studying this process. Selecting the problem initial parameters is possible to obtain a very good coincidence between the development of cyclogenesis simulation and the observed data for large-scale vortices measurements.

Space Weather Effects in Atmospheric Electric Field Variations

Kleimenova N.¹, Michnowski S.², Odzimek A.², Kubicki M.²

¹ Institute Physics of the Earth RAS, Moscow, Russia

² Institute of Geophysics PAS, Warsaw, Poland

The vertical atmospheric electric field (E_z) near the Earth surface under fair weather represent the state of the global atmospheric electric circuit, which is controlled mainly by the world thunderstorm and shower clouds activity. However, magnetosphere-ionosphere disturbances could influence this state as well. Here we present our main results of the study of the E_z effects caused by geomagnetic storms and substorms representing an important factor of the space weather. Our results are based of the E_z observations at the high-latitude station Horsund (Spitsbergen) and mid-latitude station Swider (near Warsaw, Poland). For the first time, the effect of the magnetic storm, associated with the coronal mass ejections, was revealed in the mid-latitude atmospheric electricity as the strong daytime E_z negative anomalies in relation with night-side magnetosphere substorms. However, at the polar latitudes, the auroral magnetic substorms lead to the simultaneous E_z deviations which were positive in the local morning and negative in the evening according to the station location relative to the positive or negative center of the ionosphere convection vortex. Moreover, it was found the relationship between the occurrence of the daytime E_z variations near the open/closed field line boundary and an enhancement of the region 1 field aligned currents (FAC). Thus, ground-based E_z recordings could be one of the very sensible tools to study solar wind-magnetosphere-ionosphere-atmosphere interactions.

Long-term trends in the stratosphere

Kozubek, M.

Institute of Atmospheric Physics, Czech Academy of Sciences

The long-term trend of different atmospheric parameters has been studied separately during previous years in many papers. This study is focused on the temperature, wind (u and v component), geopotential height and water vapour trends during 1979-2016. We present the trend for each month with respect to ozone turnaround during mid 1990s. The different reanalyses (MERRA, ERA-Interim, JRA-55 and NCEP-NOE) are used for comparison. We analyzed every grid point to reduce the problem with zonal averages in different pressure levels. The results will show the complex view on the trend in the middle atmosphere (troposphere, stratosphere and lower mesosphere). This comparison can give us the clue which reanalysis is better for studying different phenomena (QBO, NAO, ENSO, etc.) and which one has some issues.

Characteristic changes in the temperature of the atmosphere for different periods of time in the region of Stara Zagora

Tashev V., Manev A.

Space Research and Technologies Institute - BAS, Stara Zagora, Bulgaria

To trace the temperature of the atmosphere variation using data obtained from sensors on weather station Vantage Pro 2 Plus. The temperature of the atmosphere is determined by the difference of the amount of heat which heats the air and the amount of heat which cools the air. In this development is examined the thermal dynamics without taking into account the contributions of the individual factors. The data collected from the sensors are processed, averaged and ranked by hours, days, months and years. The results obtained are shaped in graphical and tabular form. The purpose of the study is to trace how big is a repetition in different periods. Monitoring is performed in the region of Stara Zagora.

Transient variations in global electrical circuit caused by different factors and their relation to cloud formation

Tonev P.

Space Research and Technologies Institute BAS, Sofia, Bulgaria

Transient variations of electrical characteristics in global electrical circuit (GEC) relate to intense lightning discharges, or to outer factors such as solar proton events (SPE) which cause modifications of atmospheric conductivity. These transient disturbances mostly concern the ionospheric potential, as well as the electric current and fields generated at different altitudes and latitudes by fair-weather conditions. At cloud top level they are involved in cloud formation nonlinear processes. They also may play role in regions of relatively reduced conductivity, such as mesospheric noctilucent clouds or stratospheric clouds at high latitudes. Estimations of GEC transient variations are made by two types of agents: i) intense cloud-to-ground lightning discharges (ICGLD); ii) moderate SPEs which cause conductivity changes in stratosphere and above. Computations are made for quasi-electrostatic conditions by means of modeling based on relevant equivalent electrical circuit. ICGLD can cause non-negligible (up to tenths of percent) transient change of ionospheric potential at timescale ~ 100 s, to significant changes (up to several percent) of the fair-weather electric current and field in mesospheric noctilucent clouds with highly reduced conductivity, and to several tenths of percent at cloud-top altitudes 6 - 10 km. The effects of moderate SPEs on GEC significantly differ depending on specific

Ninth Workshop

Sunny Beach, Bulgaria, May 30 - June 3, 2017

characteristics of SPE and conditions of conductivity generation. Specific examples are considered by expressed latitudinal differences of effects of SPE to conductivity related to considerable transient disturbances of electrical characteristics of GEC exceeding by many times of magnitude those caused by ICGLD.

Comparative analysis of short-term effects of solar and galactic cosmic rays on the lower atmosphere circulation in the Northern hemisphere

Veretenenko S.

Ioffe Physical-Technical Institute RAS, St. Petersburg, Russia

A comparative analysis of short-term effects of solar and galactic cosmic rays on the lower atmosphere circulation at extratropical latitudes of the Northern hemisphere was carried out. It was shown that most pronounced effects of cosmic ray variations, both solar and galactic, on the evolution of baric systems are observed in the North Atlantic region where low thresholds of geomagnetic cutoff take place allowing precipitation of particles with minimal energies from ~100 MeV to ~2-3 GeV. Depending on precipitating particle energies, intensification of baric systems occurs at high-latitudinal Arctic fronts or Polar fronts of middle latitudes. Solar proton events, with particle energies above 90 MeV, contribute to more intensive cyclone regeneration near the south-eastern coasts of Greenland where Arctic fronts are usually formed. Forbush decreases of more energetic galactic cosmic rays contribute to the intensification of blocking anticyclones at Polar fronts over the eastern North Atlantic, Northern Europe and the European territory of Russia. Importance of ionization changes due to cosmic ray variations for the physical mechanism of solar-atmospheric links was shown.

Data Processing and Modelling

Strong surfatron acceleration of helium nucleus by the electromagnetic wave in space plasmas

Erokhin N.S.^{1, 2}, Shkevov R.³, Mikhailovskaya L.A.¹, Zolnikova N.N.¹, Artekha S.A.¹

¹ Space Research Institute Russian Academy of Sciences, Moscow, Russia

² Peoples Friendship University of Russia, Moscow, Russia

³ Space Research and Technology Institute - Bulgarian Academy of Sciences, Sofia, Bulgaria

Based on numerical calculations for the wave phase on the trajectory of helium nucleus it is considered the interaction of an electromagnetic wave with the particle when the wave propagates across the magnetic field in space plasma. It was studied the conditions for the capture of helium nuclei by a wave with ultrarelativistic surfatron acceleration. Optimal conditions for the realization of strong surfatron acceleration of helium nucleus was determined. The ultrarelativistic acceleration take place in a calm space plasma in the absence of extreme events like supernova explosions. The process of surfing acceleration will provide variability of cosmic rays (CR) spectra observed by spacecraft devices. Due to the surfing mode acceleration, a small fraction of nuclei (of the order of a percent or less) has increased energy by three to five orders of magnitude. The growth of nucleus energy of CR flux, in comparison with their initial ones can increase by tens, hundred and more percent. The phenomenon can result to the appearance of a strong temporal excess in the observed CR spectrum of ultrarelativistic nucleus.

On-line catalogues of solar energetic protons at SRTI-BAS

Miteva R, Danov D.

Space Research and Technology Institute – BAS, Sofia, Bulgaria

We present the current status of activities on the on-line cataloguing of solar energetic proton events performed at the Space Climate group in the Space Research and Technology Institute - Bulgarian Academy of Sciences (SRTI-BAS). At present, the proton catalogues cover the period 1996-2016 and contain information on the identified proton events (using several satellites) as well as their solar origin. The proton catalogues are planned to be updated on yearly basis. The aim of this report is to demonstrate the structure, contents, and capabilities of the on-line catalogues: completed, in progress and planned. A dedicated web-site to host all results is set up at: <http://newserver.stil.bas.bg/SEPcatalog/>

Identification of features in solar ALMA images and comparison with solar atmospheric models

Skokic I.¹, Brajsa R.², Sudar D.², Kuhar M.³, Benz A.O.³

¹ ASU CAS Ondrejov; ² Hvar Obs. Zagreb; ³ FHNW Windisch

The Atacama Large Millimeter/submillimeter Array (ALMA) recently started with regular solar observations delivering both single-dish and interferometric images of the Sun. In these ALMA solar maps, various absorption and emission features are visible. The identified features are compared with the SDO/AIA/HMI EUV and visible light images and magnetograms, as well as with H-alpha and helium 1083 nm images from ground-based observatories. The brightness temperature of the features is measured and compared with the calculated ones. Various solar atmospheric models are used and the thermal bremsstrahlung is considered as the dominant radiation mechanism at millimeter wavelengths.

Determination of the total ozone column based on multi-dimensional lookup tables

Werner R.¹, Petkov B.², Valev D.¹, Atanassov A.¹, Guineva V.¹, Kirillov A.³

¹ Space Research and Technology Institute, BAS, Stara Zagora, Bulgaria

² Institute of Atmospheric Sciences and Climate (ISAC), CNR, Bologna, Italy

³ Polar Geophysical Institute (PGI), Apatity, Russia

Since February 2015 a Global Ultraviolet (GUV) instrument is operating regularly at the Stara Zagora observatory. The instrument measures the scattered from the sky irradiances at six wavelengths in the ultraviolet spectral region. The daily total ozone columns (TOC) were retrieved based on the ratio of two wavelengths. One of them is located in an absorption maximum of ozone. The other one is in an absorption minimum. The TOC was determined using a previously calculated lookup (Stamnes) table using the radiation transfer Tropospheric Ultraviolet and Visible (TUV) model. The influence of fast changing signal by clouds was reduced by signal smoothing and determination of the upper envelope of the time series established as function of the irradiance ratios depending of the time. Here we present an improvement of our data processing procedure using multi-dimensional lookup table, where beside the TOC, the zenith angle and the observed irradiance ratio, the effective cloud optical thickness was included as additional parameter. By help of the TUV model the ratios of the irradiance at 380 nm depending on the optical thickness and the irradiance at the same conditions but without clouds were simulated. The ratios were experimentally estimated using irradiance measurements at the wavelength channel 380 nm and measurements at the same channel during cloudless days. In the presentation the data processing is described in detail and the results obtained by the previous algorithm are shown in comparison with the improved data processing.

Instrumentation for Space Weather Monitoring

Experiment Liulin-5: Review of the Measured Radiation Characteristics on Board the International Space Station

Semkova J.¹, Koleva R.¹, Bankov N.¹, Malchev St.¹, Krastev K.¹, Benghin V.², Shurshakov V.²

¹ SRTI-BAS, Sofia, Bulgaria

² IMBP-RAS, Moscow, Russia

The radiation field around the Earth is complex, composed of galactic cosmic rays, trapped particles of the Earth's radiation belts, solar energetic particles, albedo particles from Earth's atmosphere and secondary radiation produced in the space vehicle shielding materials around the biological objects. Dose characteristics in near Earth and space radiation environment also depend on many other parameters such as the orbit parameters, solar cycle phase and current helio-and geophysical conditions. Since June 2007 the Liulin-5 charged particle telescope has been observing the radiation characteristics in two different modules of the International Space Station (ISS). In the period from 2007 to 2009 measurements were conducted in the spherical tissue-equivalent phantom of MATROSHKA-R project located in the PIRS module of ISS. From 2012 to 2015 measurements were conducted in and outside the phantom located in the Small Research Module of ISS. In this paper attention is drawn to the obtained results for the dose rates, particle fluxes and dose equivalent rates in and outside the phantom from the galactic cosmic rays, trapped protons and solar energetic particle events which occurred in that period.

Temporal offsets between solar flare index and cosmic rays

Özgül A., İsik S.

Bogazici University, Kandilli Observatory, Istanbul, Turkey

23 and 24 solar cycles flare index values and cosmic ray values are used in this study. Flare index data is taken from Kandilli observatory in Turkey, and cosmic ray data is taken from Oulu observatory in Finland. We have found very good correlations between in these two data sets. Hysteresis effect is seen during the two cycles

Role of plasmoids in magnetic reconnection: Models and observations

Barta M.¹, Skala J.^{1,2}, Karlicky M.¹, Buechner J.²

¹ Astronomical Institute ASCR, Ondrejov, Czech Republic

² Max Planck Institute for Solar System Research, Goettingen, Germany

Magnetic reconnection is now almost unanimously considered to be a key plasma process for energy release in solar and stellar flares. Recent decade have seen rapid development in the theory, simulations and searching for observational evidences of magnetic reconnection being in action in the core of flares. Modern modeling approach involves many realistic aspects of magnetic reconnection such as intrinsically 3D nature of the process and, namely, its highly dynamic character connected with violent formation of plasmoids at many scales. The cascade of plasmoid formation represents natural process of fast, turbulent energy transfer to the kinetic dissipation scale. This concept, revealed by numerical simulations, has found its ground in the theory of (ideal) plasmoid instability in current layers with high aspect ratio. The plasmoid dominated reconnection regime is capable to account for many puzzling dilemmas in the flare physics ranging from the observation-demanded energy release rate vs. standard reconnection-regime timescales, observed organized large-scale structures vs. signatures of fragmented energy release etc. The talk aims at reviewing recent theoretical and simulation development in this direction and observational support for the concept of plasmoid-driven reconnection cascade namely in solar flares.

Solar research with ALMA: Czech node of European ARC as your user-support infrastructure.

Barta M., Skokic I., Brajsa R. and the Czech ARC-node team

European ALMA Regional Center - Czech node, Astronomical Institute ASCR, Ondrejov

ALMA (Atacama Large Millimeter/sub-millimeter Array) is by far the largest project of current ground-based observational facilities in astronomy and astrophysics. It is built and operated in the world-wide cooperation (ESO, NRAO, NAOJ) at altitude of 5000m in the desert of Atacama, Chile. Because of its unprecedented capabilities, ALMA is considered as a cutting-edge research device in astrophysics with potential for many breakthrough discoveries in the next decade and beyond. In spite it is not exclusively solar-research dedicated facility, science observations of the Sun are now possible and will started in the current observing Cycle 4 (2016-2017).

In order to facilitate user access to this top-class, but at the same moment very complicated device to researchers lacking technical expertise, a network of three ALMA Regional Centers (ARCs) has been formed in Europe, North America, and East Asia as a user-support infrastructure and interface between the observatory and users community. After short introduction to ALMA the roles of ARCs and hint how to utilise their services will be presented. Finally, peculiarities of solar observations that demanded the development of the specific Solar ALMA Observing Modes will be discussed and the results of Commissioning and Science Verification observing campaigns (solar ALMA maps) will be shown.

**The particularity of investigation of ELF-VLF
electromagnetic radiation on sun-synchronous orbits.
Project RELEC/Vernov.**

*Klimov S.¹, Grushin V.¹, Novikov D.¹, Belyakova L.¹, Osadchaya L.¹,
Ferencz Cs.², Szegedi P.², Korepanov V.³, Belyayev S.³, Marusenkov A.³,
Kirov B.⁴, S. Asenovski S.⁴, Georgieva K.⁴*

¹ Space Research Institute of the RAS, Moscow, Russia

² Eötvös University, Budapest, Hungary

³ Lviv Centre of Institute of Space Research NAN-NSA, Lviv, Ukraine

⁴ SRTI-BAS, Sofia, Bulgaria

The program of physical studies on the Vernov satellite launched on July 8, 2014 into a polar (640 × 830 km) solar-synchronous orbit with an inclination of 98.4° is presented. We described the complex of scientific equipment on this satellite in detail. We compare the Vernov data with the ones from the Obstanovka experiment aboard the International Space Station.

**Comparison of Vertical Ionospheric Drifts Obtained by
Different Techniques**

Kouba, D.

Institute of Atmospheric Physics, Czech Academy of Sciences

Since 2004 the ionospheric observatory in Pruhonice (Czech Republic, 50N, 14.9E) provides regular ionospheric sounding using Digisonde. In addition to classical ionograms the drift velocities in both E and F region using DDA method are measured routinely.

However, vertical component of the drift velocity vector can be estimated by several different methods which can be found in the literature; for example the indirect estimation based on the temporal evolution of measured ionospheric characteristics is often used for calculation of the vertical drift component. The vertical velocity is thus estimated according to the change of characteristics scaled from the classical quarter-hour ionograms.

In present paper the direct drift measurement is compared with technique based on measuring of the virtual height at fixed frequency from the F-layer trace on ionogram, technique based on variation of h'F and hmF. The ionospheric observatory in Pruhonice is midlatitudinal station and typically provides measurements in 15 minutes cadence. Due to the fact that the most papers use different indirect methods use equatorial data, we also focus on results of equatorial stations and other stations that carry out measurements with higher cadence (5 minutes).

Our comparison shows possibility of using different methods for calculating vertical drift velocity and their relationship to the direct measurement used by Digisonde.

Presentation of the book "Life and Universe"

Obridko V.

IZMIRAN Moscow, Russian

One of the most fundamental problems in science is the origin and evolution of life on the Earth. We don't even know whether the terrestrial life originated on the Earth or was brought from outside. Some of the questions needing answers in order to solve this problem are the thermal regime of the young Earth which is in turn related to the activity of the young Sun, the timing of the formation of the liquid and solid cores, the origin, structure and evolution of the Earth's magnetic field, the formation and characteristics of the atmosphere and hydrosphere. These questions were discussed during the colloquium "The Earth on the early stages of the evolution of the solar planetary system" held in November 2016 in Moscow. The monograph "Life and Universe" summarizes the results of this colloquium.

The editors of the monograph are V.Obridko and M. Ragulskaya.

Author's List

- Alisoy H. (1),
Artekha S.A. (2),
Asenovski S. (2)
Atanassov A. (1),
Atici R. (2),
Bankov N. (1),
Baranov D. (1),
Barta M. (2)
Belyaev G. (1),
Benghin V. (3),
Benz A.O. (1),
Bershadszkaya I. (1),
Besliu-Ionescu D. (1),
Belyakova L. (1)
Bojilova R. (1),
Boska J. (3),
Boychev B. (1),
Brajša R. (2),
Brazhenko A. (3),
Bubnov I. (1),
Buechner J. (1)
Canyilmaz M. (2),
Charkina O.V. (1),
Chernouss S. (1),
Chum J. (1),
Cukavac M. (1),
Dachev Ts. (1),
Danilova O. (1),
Danov D. (1),
Dechev M. (2),
Demekhov A.G. (2),
Demetrescu C. (2),
Denker C. (1),
Despirak I.V. (3),
Dimitrov P. (1),
Dineva E.I. (1),
Dobrica V. (2),
Donmez B. (1),
Dorovskyy V. (2),
Dremukhina L.A. (1),
Drobyshev S. (1),
Duchlev P. (2),
Dzhalilov N.S. (1),
Efishov I. (1),
Erokhin N.S. (2),
Ferencz Cs. (1)
Filatov M. (1),
Frantsuzenko A. (1),
Georgieva K. (4),
Golovin D. (2),
Greculeasa (1),
Gromov S.V. (1),
Gromova L. (2),
Grushin V. (1)
Guineva V. (3),
Güzel E. (1),
Hasanagić E. (1),
Huseynov S.Sh. (1),
Ilyin I. (1),
Ishkov V.N. (2),
Ishkova L. (1),
İsik S (1)
Ivantishin O. (1),
Kalinichenko N. (1),
Kaportseva K. (1),
Karlica M. (1),
Karlicky M. (1)
Kilcik A. (6),
Kirillov A. (1),
Kirov B. (4),
Kleimenova N. (4),
Klimov S. (1)
Koleva K. (2),
Koleva R. (2),
Komendant V. (1),
Konovalenko A. (3),
Korepanov V. (1)
Koshkin N. (1),
Kosovichev Al. (1),
Kostin V. (1),
Kouba D. (4),
Koucka-Knizova P. (3),
Koval A.A. (1),
Kozelov B. (1),
Kozubek M. (2),
Krastev K. (2),
Krupar V. (1),
Kubicki M. (1),
Kuhai N. (1),
Kuhar M. (1),
Kurt K. (1),
Lubchich A.A. (1),
Lukashenko A. (1),
Lytvynenko I. (1),
Lytvynenko O. (3),
Malahov A. (2),
Malchev S. (2),
Manev A. (2),
Manninen J. (1),
Maričić D. (1),
Maris-Muntean G. (1),
Marusenkov A. (1)
Matvichuk Y. (1),
Melnik V. (2),
Meshalkina N.S. (1),
Michnowski S. (1),
Mierla M. (1),
Mihajlović S. (1),
Mikhailovskaya L.A. (2),
Milenković M. (1),
Milovanović B (1),
Miteva R. (2),
Mitrofanov I. (2),
Mokrousov M. (1),
Mosna Z. (2),
Mukhtarov P. (1),
Nagovitsyn Yu. (1),
Obridko V.N. (4),
Odzimek A. (1),
Olyak M. (1),
Orlyuk M. (1),
Ovcharenko O. (1),
Ozcan O. (2),
Özgüç A. (3),
Panchenko M. (1),
Petkov B. (1),
Podgorny A.I. (2),
Podgorny I.M. (2),
Popova E. (1),
Popova T.A. (1),
Potuznikova K. (2),
Radovanović M. (1),
Romanchuk O. (1),
Romenets A. (1),
Rozelot J.-P. (2),
Roša Dr. (1),
Rucker H. (2),
Ruzhin Yu. (1),
Ryabov M.I. (4),
Rycroft M. (1),
Sahin S. (2),
Samwel S.W. (1),
Sanin A. (1),
Sarp V. (2),

Ninth Workshop
Sunny Beach, Bulgaria, May 30 - June 3, 2017

Sağır S. (7),	Czech ARC-node team (1)
Semenova N.V. (1),	
Semkova J. (3),	FREND team (2)
Sergeeva N.A. (1),	<i>Benghin V.</i>
Shagimuratov I. (1),	<i>Dachev Ts.</i>
Shepeliev V. (1),	<i>Dimitrov P.</i>
Shepherd S.J. (1)	<i>Drobyshev S.</i>
Shevchuk M. (1),	<i>Fedosov F.</i>
Shkevov R. (2),	<i>Golovin D.</i>
Shurshakov V. (2),	<i>Grebennikova N.</i>
Sindelarova (1),	<i>Koleva R.</i>
Skala J. (1)	<i>Kozyrev A.</i>
Skokic I. (2),	<i>Krastev K.</i>
Stanislavsky A.A. (1),	<i>Litvak M.</i>
Strassmeier K.G. (1),	<i>Malahov A.</i>
Sudar D. (1),	<i>Maltchev St.</i>
Sukharev A.L. (3),	<i>Matviichuk Yu.</i>
Szegedi P. (1)	<i>Mitrofanov I.</i>
Tashev V. (2),	<i>Mokrousov M.</i>
Tepenitsyna N. (1),	<i>Nikiforov S.</i>
Tomov B. (1),	<i>Sanin A.</i>
Tonev P. (1),	<i>Semkova J.</i>
Trushkina E. (1),	<i>Shurshakov V.</i>
Tsvetkov Ts. (1),	<i>Tomov B.</i>
Petrov N. (1),	<i>Tretyakov V.</i>
Turunen T. (1),	<i>Vostrukhin A.</i>
Tyasto M. (2),	
Valev D. (1),	
Veretenenko S. (1),	
Vernova E. (2),	
Veselovsky I. (1),	
Volvach A.E. (1),	
Volvach Ya.S. (1),	
Werner R. (3),	
Yahnin A.G. (2),	
Yahnina T.A. (1),	
Yampolski Yu.M. (1),	
Yankova Kr. (1),	
Yaşar M. (2),	
Yerin S. (1),	
Yesil A. (4),	
Yurchyshyn V. (2),	
Zabarinskaya L.P. (1),	
Zalizovski A.V. (1),	
Zharkov S.I. (1),	
Zharkova V.V. (1),	
Zolnikova N.N. (2),	

Ninth Workshop
Sunny Beach, Bulgaria, May 30 - June 3, 2017